Biomolecular Conformations can be Identified as Metastable Sets of Molecular Dynamics.

Christof Schütte, * Wilhelm Huisinga [1]

Institute of Mathematics II, Department of Mathematics and Computer Science, Free University (FU) Berlin, Germany

Abstract

This article summarizes the present state of the transfer operator approach to biomolecular conformations with special emphasis on the conceptual and mathematical foundations.

Key words: conformation analysis, Markov process, transfer operator, exit rate, transition probability, dominant eigenvalues, canonical ensemble, stationary ensemble, short–term trajectories, long–term simulation

* Corresponding author
Email addresses: schuette@math.fu-berlin.de (Christof Schütte,), huisinga@math.fu-berlin.de (Wilhelm Huisinga).
URLs: www.math.fu-berlin.de/~biocomp (Christof Schütte,), www.math.fu-berlin.de/~huisinga (Wilhelm Huisinga).

[1] Supported by the Deutsche Forschungsgesellschaft (DFG) within the priority research program "Analysis, Modeling and Simulation of Multiscale Problems".

Chapter 1. Introduction

The biochemical functions of many important biomolecules result from their *dynamical* properties, particularly from their ability to undergo so-called *conformational transitions* (cf. [64]). In a conformation, the large scale geometric structure of the molecule is understood to be conserved, whereas on smaller scales the system may well rotate, oscillate or fluctuate. Furthermore, transitions between conformations are rare events or, in other words, a typical trajectory of a molecular system stays for long periods of time within the conformation, while exits are long-term events. Hence, the term conformation includes both geometric and dynamical aspects. From the geometrical point of view, conformations are understood to represent all molecules with the same large scale geometric structure and may thus be identified with a subset of the state space. From the dynamical point of view, a conformation typically persists for long periods of time (compared to the fastest molecular motions) such that the associated subset of the state space is *metastable* and the resulting *macroscopic dynamical behavior* can be described as a flipping process between the metastable subsets.

Understanding *conformation dynamics*—that is the statistics of the flipping process and the corresponding exit times as well as the actual transition paths between different conformations—is crucial to the understanding of biomolecular flexibility and activity. Prominent examples of conformation dynamics are the conformational changes accompanying the action of the muscle protein myosin, the light-induced conformational transition of the photo-receptor rhodopsin initializing the primary amplification cascade in vision, or the conformation conversion of human prions assumed to cause prion diseases.

The state–of–the–art biophysical explanation for the existence of conformations is as follows: The *free energy landscape* of a protein or peptide decomposes into particularly deep wells each containing huge numbers of local minima. These wells are separated by relatively large barriers—as measured on the scale of the thermal energy k_BT—from each other and represent different metastable conformations. The hierarchy of barrier heights induces a hierarchy of conformations [21, 27, 26]. The corresponding hierarchy of time scales observed for conformational transitions seems to confirm the biophysical explanation for the existence of conformations [49]. However, the entire explanation depends on the concept of the free energy landscape, whose definition is typically based on the assumption that the conformational degrees of freedom are already known in advance. In other words, the model is of minor use if conformations and conformational degrees of freedom still have to be identified by simulations.

Mathematically, the dynamical aspect of conformations is based on the concept of metastability. In this paper we will pursue two characterizations of

metastability. The *Exit Time Approach* based on *exit rates* characterizes metastability of some subset by the property that a typical trajectory will only exit the subset on macroscopically long time scales. The *Ensemble Dynamics Approach* based on *transition probabilities* characterizes metastability of some subset in statistical terms in the following sense: the fraction of systems in an ensemble that exit from the subset during some (not necessarily long) given time span is significantly small in comparison to other subsets. It is one of the main goals of this article to discuss and compare the similarities and distinguishing aspects of these two concepts in detail (the entire Chapter 2 will be devoted to the conceptual differences).

We will see that the two characterizations of metastability can be formalized and studied within the unified mathematical framework of the *transfer operator approach* to metastability. This approach originated from the work of Dellnitz et al. on the identification of almost invariant sets of discrete dynamical systems with small random perturbations [13, 11] and it has been successfully applied to examine metastable behavior of deterministic Hamiltonian systems by Deuflhard et al. [13]. By reformulating this idea in the context of biophysical models of molecular motion, Schütte et al. showed that biomolecular conformations can be identified via the "dominant" eigenvectors of the transfer operator associated with the dynamical model used [55, 57, 54, 35]. It has been demonstrated that, for moderate size (bio)molecules, the eigenvectors of interest can be computed efficiently and allow to identify the desired conformations and the associated conformation dynamics in a unified setting based on simulation of the dynamical behavior of molecular systems [25, 17, 38].

The literature on conformation dynamics is enormously rich, see e.g., [15, 3]. However, the branch that deals with the *dynamical* aspects of conformations mainly contains approaches to the computational detection of transition paths between conformations and of the associated main transition coordinates, see [20, 27, 5]. There are several approaches designed to bridge the time scale gap between realizably short trajectory simulations and significantly longer metastability periods of conformational substates. One example are approaches that exploit artificial accelerations of the dynamics, cf. [32, 34]; another example is given by path integral approaches to long–term dynamics where transition paths are discretized in time using extremely large timesteps [50].

The article will be organized as follows: First we will sharpen and conceptually complement the two characterizations of metastability (Chapter 2), then we will shortly summarize the different dynamical models designed to describe different aspects of the dynamical and statistical properties of molecules (Chapter 3). This will be followed by the presentation of the mathematical framework of the transfer operator approach to metastability (Chapters 4 and 5). Within this framework we will reformulate the two concepts of metastabil-

ity and justify in detail the key idea of the transfer operator approach. Moreover, it will be shown that the framework allows to incorporate almost all different dynamical models available. In Chapter 6 the theoretical level is left and the issues of practical realization are discussed: The concept of Galerkin discretization of transfer operators is studied which leads to the question of whether a discretization of the eigenvalue problem in huge dimensional state spaces will be possible without risking the increase of numerical effort beyond any tolerable amount. It is illustrated how this problem can be circumvented. Chapters 7 and 8 conclude the article by demonstrating the application of the approach. In Chapter 7 the entire concept is illustrated by means of a simple but completely comprehensible test system whereas Chapter 8 is devoted to the application to a small oligonucleotide.

Chapter 2. Conceptual Preliminaries

Before we go into details about molecular dynamics, conformations, and metastability we first want to point out the fundamental principles of the approach to biomolecular conformations.

Let us assume for the remainder of this section that a mathematical model is available which, given an exact initial state, perfectly describes the true motion of the molecule under consideration in all necessary details. In general, this will be given by some (discrete or continuous, deterministic or stochastic) dynamical system. In the deterministic setting, the corresponding initial value problem is thought to model the evolution of the state of a *single molecule*; its exact solution will be called "trajectory" in the following. In the stochastic setting, we use the same interpretation and wording for every single pathwise realization. Trajectories have to be distinguished from their numerical realization, which will be called "simulation" or "numerical integration".

In the context of biochemical applications one is generally not interested in single isolated molecules but in certain *molecular ensembles* that, for instance, model the collection of many identical molecules in a living cell or in a test tube with certain side conditions like, e.g., constant temperature. The molecular ensemble is represented by a statistical distribution in molecular state space. If the ensemble is assumed to be stationary, the distribution does not change in time (see Figure 1). Within this setting, the *transition probability* from some sub–ensemble A to some sub–ensemble B, both specified by some subset A and B of the state space, within a pre–described time span τ is given by the fraction of systems with initial state in A at $t = 0$ and final state in B at $t = \tau$. Built upon transition probabilities we may state the

Ensemble Dynamics Approach: Conformations are identified as sub–ensembles/subsets, for which the fraction of systems that exit during a

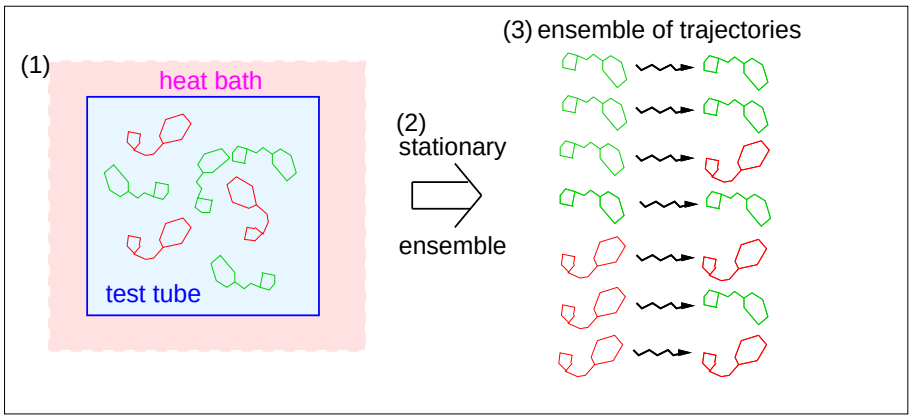

Fig. 1. *Illustration of ensemble dynamics: (1) an ensemble of molecular systems embedded in a heat bath of constant temperature; (2) the usual assumption is that this can be modeled by some stationary probability distribution, e.g., the canonical density; (3) the dynamical behavior of each single molecule in the ensemble (here assumed to be modeled accurately by some dynamical system with flow Φ^τ) induces dynamical fluctuations within the ensemble without effect on the stationary distribution.*

prescribed observation time τ is significantly smaller than for other sub–ensembles/subsets.

In order to numerically *compute* the transition probabilities from sub–ensemble A to B one has to generate (i) a sample that represents the *sub–ensemble of initial states* in A, and (ii) a sample that represents the corresponding *sub–ensemble of trajectories* starting from these initial states, as illustrated in Figure 1. Within this statistical setting the ensemble dynamics approach is able to capture conformation dynamics by considering only *short–term* trajectories, since measurements on ensembles already contain information about all possible states, and short–term trajectories over time spans that are of the order of magnitude of the rapid conformational transition itself contain all transition paths from one conformation to another.

The ensemble dynamics approach has the advantage that it is based on a setting and requires information which is experimentally available: ensembles of short-term trajectories can be observed by means of femtochemistry (Nobel price 1999) [62, 63], a novel technique that permits us to observe the dynamical behavior of molecular systems in real–time. Boosted by the progress in laser technology, ultrashort light pulses can be generated with durations on the typical timescales of molecular vibrations, i.e., from picoseconds down to femtoseconds. The prototypical experiment follows the *pump–probe scenario*: A molecular ensemble that is initially prepared in some stationary state is excited by a first laser pulse ("*pump*") thus lifting the system into an excited state. Subsequently, a second laser pulse ("*probe*") is used to stimulate another transition (emission or absorption) that serves to generate an observable signal. By measuring the observable signal as a function of the time delay

between pump and probe pulse the evolution of the system in its excited state can be monitored. Hence, pump–probe measurements allow to experimentally realize the ensemble dynamics approach.

In this article we will present two different algorithmic approaches to generate the data needed in steps (i) and (ii) from above. The two concepts are sketched in Figure 2. On the one hand, we may use *any* method available to compute a sample that appropriately represents the stationary distribution. Given this sample one then evaluates the trajectories starting from any sample point. We will see later that the two steps may be combined into a single procedure by introducing an appropriate Markov chain. On the other hand, whenever the dynamical system under consideration is *ergodic* [2], a single long–term trajectory represents the average behavior of molecules in the ensemble. Then, chopping the long–term trajectory into pieces of length τ will also do the job.

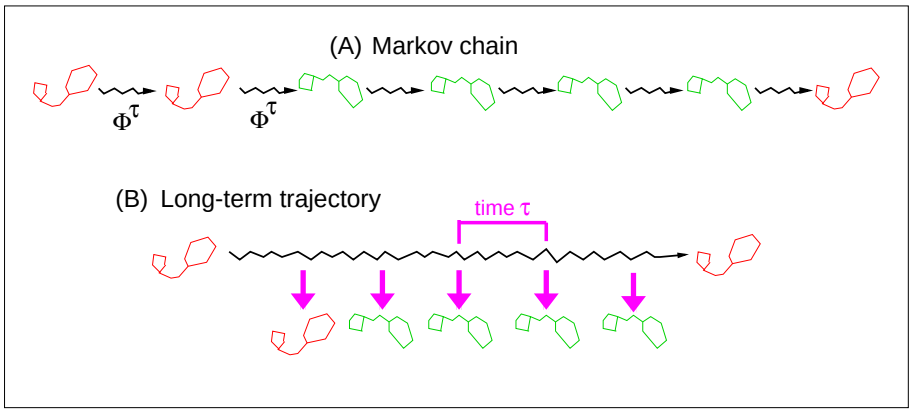

Fig. 2. *Illustration of different algorithmic options for realizing a sample of the stationary ensemble under consideration and the induced sample the corresponding ensemble of trajectories: realization of ensemble and trajectories can be done by means of (A) specially designed Markov chains, or (B) time-τ pieces from a single ergodic long-term simulation of the corresponding dynamical system.*

This algorithmic option via long–term simulation should not be confused with another approach to conformation analysis, the

> **Exit Time Approach**: Conformations are identified as subsets for which the exit time of a typical trajectory is extraordinary large in comparison to other subsets.

This approach is build upon the belief that the description of conformational transitions requires to start a long–term simulation and wait through the in general tremendously long period of time until a transition takes place. However, as we will see in the following this is not necessarily the case, and

[2] The notion of ergodicity has several different meanings in physics and mathematics. The typical rough "definition" states that "time average equals ensemble average". We will introduce the precise meaning used in this article in Section 7.

the notion of conformations in the ensemble dynamics and exit time approach in some sense turn out to be very similar.

Both approaches may exploit long–term *simulations* in the ergodic interpretation in order to generate ensembles of short–term trajectories only. Yet, the authors want to emphasize that long–term *trajectories* of the dynamical system under consideration are not necessarily needed. This is of utmost importance because the literature on predictability and sensitivity w.r.t. perturbations states that for any dynamical system and prescribed accuracy there is a certain maximal time T, up to which initial value problems are make sense. For time spans longer than T the deviation between trajectories of the dynamical system caused by perturbations may exceed the accuracy requirement. The nature of the perturbations to be considered depends on the actual application context: one may have to take into account the uncertainty of the initial value, or perturbations due to the numerical realization. The actual value of T depends on the properties of the dynamical system and on the nature of the perturbations and can be characterized by means of different estimates (e.g. by Lyapunov exponents, so–called condition numbers [12], or predictability analysis [42]). However, in the context of biomolecular dynamics all available estimates indicate that for any tolerable accuracy, the time T is many orders of magnitude smaller than the expected exit times from typical conformations. The same situation is encountered in the above mentioned pump–probe experiments, where the time spans between the pump and probe pulse are orders of magnitude smaller than typical exit times from some conformation. However, experimental observations of conformational transitions in real-time over milliseconds or even on longer scales are very limited and possible only indirectly.

Before proceeding to the algorithmic realization of the ensemble dynamics or exit time approach we may first introduce the most prominent types of dynamical systems presently discussed in the context of molecular dynamics. They can be classified in two main categories:

(MC1) Dynamical systems that are designed to model the precise motion of some molecular system, at least on short time scales.

(MC2) Dynamical systems that are designed to sample the state space of some molecular system w.r.t. some prescribed statistical distribution.

Chapter 3. Description of Dynamical Behavior

The literature on the description of the dynamical behavior of molecular systems is extremely rich; they range from classical deterministic Hamiltonian models that try to cover the actual motion of each single molecule in the system to stochastic descriptions like Langevin dynamics or iterative schemes

that only model artifical dynamics like most Markov chain Monte Carlo approaches.

1 Markov Processes and Transition Functions

We now introduce the mathematical framework that subsumes both approaches, whether stochastic or deterministic.

Consider the state space $\mathbf{X} \subset \mathbf{R}^m$ for some $m \in \mathbf{N}$ equipped with the Borel σ–algebra $\mathcal{A}$ on $\mathbf{X}$.[3] The evolution of a single microscopic system is supposed to be given by a **homogeneous Markov process** $X_t = \{X_t\}_{t \in \mathbf{T}}$ in continuous or discrete time $\mathbf{T} = \mathbf{R}_0^+$ or $\mathbf{T} = \mathbf{N}$, respectively. We write $X_0 \sim \mu$, if the Markov process X_t is initially distributed according to the probability measure μ, i.e., if $\mathbf{P}[X_0 \in A] = \mu(A)$ for every $A \subset \mathbf{X}$. We use $X_0 = x$, if $X_0 \sim \delta_x$, where δ_x denotes the Dirac measure at x. The motion of X_t is given in terms of the **stochastic transition function** $p : \mathbf{T} \times \mathbf{X} \times \mathcal{B}(\mathbf{X}) \to [0, 1]$ according to

$$p(t, x, A) \;=\; \mathbf{P}[X_{t+s} \in A \;|X_s = x], \tag{1.1}$$

for every $t, s \in \mathbf{T}$, $x \in \mathbf{X}$ and $A \subset \mathbf{X}$. Hence, $p(t, x, A)$ describes the probability that the system moves from state x into the subset A within time t. The relation between a stochastic transition function and a homogeneous Markov process is one–to–one [48, Chapter 3]. In the special case, where $p(t, x, A) = \delta_{\Phi(x,t)}(A)$, the Markov process is in fact a deterministic process, whose evolution is defined by the flow map $\Phi(x, t)$ in state space. Besides some more technical properties (see Appendix A) the stochastic transition function fulfills the so–called Chapman–Kolmogorov equation

$$p(t + s, x, A) \;=\; \int_{\mathbf{X}} p(t, x, \mathrm{d}z)\; p(s, z, A) \tag{1.2}$$

that holds for every $t, s \in \mathbf{T}$, $x \in \mathbf{X}$ and $A \subset \mathbf{X}$ and represents the semigroup property of the Markov process. As a consequence, in the discrete time case $\mathbf{T} = \mathbf{N}$ it suffices to specify $p(x, \mathrm{d}y) = p(1, x, \mathrm{d}y)$, since the n–step transition probabilities $p^n(x, \mathrm{d}y) = p(n, x, \mathrm{d}y)$ are recursively determined by (1.2).

We say that the Markov process X_t admits an **invariant probability mea-**

[3] In the sequel every subset $C \subset \mathbf{X}$ is implicitly assumed to be measurable, i.e., we assume that additionally $C \in \mathcal{A}$ holds without further mentioning.

sure μ, or μ is invariant w.r.t. X_t, if

$$\int_{\mathbf{X}} p(t,x,A)\mu(\mathrm{d}x) \;=\; \mu(A) \tag{1.3}$$

for every $t \in \mathbf{T}$ and $A \subset \mathbf{X}$ [48, Chapter 10]. Note that the invariant probability measure needs not to be unique. A Markov process is called **reversible** w.r.t. an invariant probability measure μ if

$$\int_A p(t,x,B)\mu(\mathrm{d}x) \;=\; \int_B p(t,x,A)\mu(\mathrm{d}x) \tag{1.4}$$

for every $t \in \mathbf{T}$ and $A, B \subset \mathbf{X}$. If μ is unique, X_t is simply called reversible. For the special case of a stochastic transition function being absolutely continuous w.r.t. μ, reversibility reads $p(t,x,y) = p(t,y,x)$ for every $t \in \mathbf{T}$ and μ–a.e. $x, y \in \mathbf{X}$.

2 Model Systems

We now turn to the most prominent examples in the context of molecular dynamics.

Let N denote the number of atoms of the system and $\Omega = \mathbf{R}^{3N}$ the position space, i.e., $q \in \Omega$ represents the vector of atomic position coordinates. Moreover, let $\xi \in \mathbf{R}^{3N}$ denote the vector of all conjugated momenta. Suppose that a differentiable potential energy function $V : \mathbf{R}^{3N} \to \mathbf{R}$ describing all interactions between the atoms is given. For each model system below we assume that the positon space Ω belongs to one of the two fundamentally different cases:

Bounded systems: The potential energy function $V : \mathbf{R}^{3N} \to \mathbf{R}^{3N}$ is smooth, bounded from below, and satisfies $V \to \infty$ for $|q| \to \infty$. Such systems are called bounded, since the energy surfaces $\{(q,\xi) \in \Gamma : H(q,\xi) = E\}$ are bounded subsets of Γ for every energy E.

Periodic systems: The position space Ω is some $3N$–dimensional torus and the potential energy function V is continuous on Ω and thus bounded. There is an intensive discussion concerning the question of whether V can also be assumed to be smooth as we will do herein, see [54, Section 2] for details.

Both cases are typical for molecular dynamics applications. Periodic systems in particular include the assumption of periodic boundaries, which is by far the most popular modeling assumption for biomolecular systems.

Deterministic Hamiltonian System. The most prominent model for the dynamical behavior of molecular systems exploits classical Hamiltonian mechanics, i.e., atoms are described as mass points subject to forces that are generated by specified classical interaction potentials V. The dynamical behavior is described by some deterministic Hamiltonian system of the form

$$\dot{q} \;=\; M^{-1}\xi, \qquad \dot{\xi} \;=\; -\nabla_q V(q), \tag{2.1}$$

defined on the state space $\mathbf{X} = \mathbf{R}^{3N} \times \mathbf{R}^{3N}$ and M denoting the diagonal mass matrix.

Eq. (2.1) models an energetically closed system, whose total energy, given by the Hamiltonian

$$H(q,\xi) \;=\; \frac{1}{2}\xi^T M^{-1}\xi \;+\; V(q), \tag{2.2}$$

is preserved under the dynamics. For the sake of simplicity, we assume in the following that M is the identity matrix. The deterministic Hamiltonian system is typically seen as the embodiment of our class (MC1) in the context of molecular dynamics.

Let Φ^t denote the flow associated with the Hamiltonian system (2.1), i.e., the solution $x_t = (q_t, \xi_t)$ of (2.1) for the initial value $x_0 = (q_0, \xi_0)$ is given by $x_t = \Phi^t x_0$. Let $\mathbf{1}_C$ denote the characteristic function of the subset $C \subset \mathbf{X}$. Then, the stochastic transition function corresponding to (2.1) is given by

$$p(t,x,C) \;=\; \mathbf{1}_C\Big(\Phi^t x\Big) \;=\; \delta_{\Phi^t x}(C) \tag{2.3}$$

for every $t \in \mathbf{R}_0^+$ and $C \subset \mathbf{X}$. The Markov process $X_t = \{X_t\}_{t\in\mathbf{R}_0^+}$ induced by the stochastic transition function p coincides with the flow Φ^t; hence $X_t = \Phi^t x_0$ for the initial distribution $X_0 = x_0$.

It is well known that for every smooth function $\mathcal{F} : \mathbf{R} \to \mathbf{R}$ the probability measure $\mu(\mathrm{d}x) \propto \mathcal{F}(H)(x)\mathrm{d}x$ is invariant w.r.t. the Markov process X_t. The most prominent choice is the canonical density or **canonical ensemble**

$$f(x) \;\propto\; \exp(-\beta H(x))$$

for some constant $\beta > 0$ that can be interpreted as inverse temperature. The associated measure $\mu(\mathrm{d}x) \propto f(x)\mathrm{d}x$ is called the **canonical measure**. The canonical ensemble is often used in modeling experiments on molecular systems that are performed under the conditions of constant volume and temperature $\mathcal{T} = \frac{1}{k_B\beta}$, where k_B Boltzmann's constant. Obviously, a single solution of the Hamiltonian system (2.1) can never be ergodic w.r.t. the canonical measure, since it conserves the internal energy H, as defined in (2.2). Hence, w.r.t. the canonical measure, the deterministic Hamiltonian system is not in

the class (MC2), while it might be w.r.t. to other measuere such as, e.g., the microcanonical measure.

Hamiltonian System with Randomized Momenta. Aiming at a conformational analysis of biomolecular systems in the context of the canonical ensemble, Schütte et al. introduced a specific stochastic Hamiltonian system [55] as a discrete time Markov chain, defined solely on the position space and derived from the deterministic Hamiltonian system by "randomizing the momenta".

For some fixed observation time span $\tau > 0$ (for comments on the choice of τ see remark below) and some inverse temperature $\beta > 0$ the stochastic transition function for the Hamiltonian system with randomized momenta is given by

$$p(q, A) \;=\; \int_{\mathbf{R}^d} \mathbf{1}_A\Big(\Pi_q \Phi^\tau(q,\xi)\Big)\mathcal{P}(\xi)\mathrm{d}\xi,$$

where $\Pi_q : (q,\xi) \mapsto q$ denotes the projection onto the position space $\Omega = \mathbf{R}^{3N}$ and $\mathcal{P}$ the canonical distribution of momenta $\mathcal{P} \propto \exp(-\beta\xi^t\xi/2)$.

The associated discrete time Markov process $Q_n = \{Q_n\}_{n\in\mathbf{N}}$, defined on the state space $\mathbf{X} = \Omega$, satisfies

$$Q_{n+1} \;=\; \Pi_q \Phi^\tau(Q_n, \xi_n); \qquad n \in \mathbf{N} \tag{2.4}$$

where ξ_n is chosen randomly from $\mathcal{P}$ [54]. As it is shown in [54] the positional canonical measure $\mu(\mathrm{d}q) \propto \exp(-\beta V(q))\mathrm{d}q$ is invariant w.r.t. Q_n and unique. Moreover, exploiting that Φ^τ is reversible and symplectic Q_n is shown to be reversible w.r.t. μ [54].

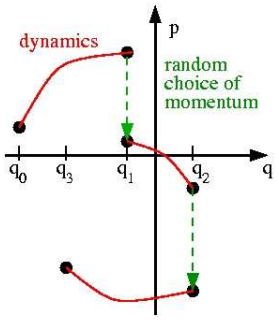

Fig. 3. *Illustration of the Hamiltonian system with randomized momenta as defined in (2.4).*

The Hamiltonian system with randomized momenta generates an ensemble of time–τ trajectories such that each trajectory follows the deterministic Hamiltonian dynamics (2.1) starting at initial values distributed according to the

positional canonical ensemble $f(q) \propto \exp(-\beta V(q))$ (see Fig. 2 for illustration). When the deterministic Hamiltonian system is beliefed to be contained in class (MC1), then the Hamiltonian system with randomized momenta is contained in the classes (MC1) *and* (MC2).

Remark. For arbitrary, but fixed $\tau > 0$ we have defined the *one–step* transition function $p(q, D) = p^\tau(1, q, D)$. Changing the observation time to $\sigma > 0$ results in a new one–step transition function $p^\sigma(1, q, D)$. In general we will have $p^{2\tau}(1, q, D) \neq p^\tau(2, q, D)$; for an example see [54, Section 3.7.1].

Constant Temperature Molecular Dynamics. One traditional aspect of molecular dynamics is the construction of (stochastic) dynamical systems that allow of sampling the canonical ensemble by means of long-term simulation. Several concepts have been discussed that all boil down to the idea to construct a Hamiltonian system in some extended state space $\hat{\mathbf{X}}$, whose projection onto the lower dimensional state space $\mathbf{X}$ of positions and momenta allows to generate such a sampling. One of the most prominent examples is defined in terms of the Nosé Hamiltonian

$$H_{\text{Nose}}(q, \xi, s, \nu) \;=\; \underbrace{\frac{1}{2s^2}\xi^T\xi \;+\; V(q)}_{=H_s(q,\xi)} \;+\; \frac{1}{2Q}\nu^2 \;+\; \frac{1}{\beta}\log s,$$

where s is called the thermostat with conjugated momentum π and associated artificial mass Q. Let the flow of the associated Nosé Hamiltonian system be denoted Ψ^t and let Π denote the projection $(q, \xi, s, \nu) \mapsto (q, \xi)$. If Ψ^t is ergodic w.r.t. the microcanonical measure on the associated energy cell of H_{Nose}, then $\Pi\Psi^t$ is ergodic w.r.t. the canonical measure $\mu(\mathrm{d}x) \propto \exp(-\beta H_{s=1}(x))\mathrm{d}x$, where $x = (q, \xi)$ [6]. Thus, the Nosé Hamiltonian system is contained in the class (MC2) but it is at least questionable whether it is part of (MC1).

Langevin System. The most popular model for an *open system* with stochastic interaction with its environment is the so-called Langevin System [52]:

$$\dot{q} \;=\; \xi, \qquad \dot{\xi} \;=\; -\nabla_q V(q) \;-\; \gamma\,\xi \;+\; \sigma\,\dot{W}_t, \tag{2.5}$$

defined on the state space $\mathbf{X} = \mathbf{R}^{6N}$. Here $\gamma > 0$ denotes some friction constant and $F_{\text{ext}} = \sigma\dot{W}_t$ the external forcing given by a $3N$-dimensional Brownian motion W_t. The external stochastic force is assumed to model the influence of the heat bath surrounding the molecular system. In this case, the internal energy given by the Hamiltonian H, as defined in (2.2), is not preserved, but the interplay between stochastic excitation and damping balances the internal energy. As a consequence, the canonical measure $\mu(\mathrm{d}x) \propto \exp(-\beta H(x))\mathrm{d}x$ with $x = (q, \xi)$ is invariant w.r.t. the Markov process corresponding to the

Langevin system, where the noise and damping constants satisfy [52]:

$$\beta \;=\; \frac{2\gamma}{\sigma^2}. \tag{2.6}$$

Thus, the Langevin system satisfies our expectation on (MC2) w.r.t. the canonical ensemble but simultaneously also allows to represent some essential aspects of (MC1), i.e., of the true dynamical behavior of the molecular system. For more details see article of Tamar Schlick in this handbook.

Smoluchowski System. The Smoluchowski system can be understood as an approximation to the Langevin system in the limit of high friction $\gamma \to \infty$, see [35, 56] for details. While the Langevin system gives a description of molecular motion in terms of positions and momenta of all atoms in the system, the Smoluchowski system is stated in the position space only. Moreover, in contrast to the Langevin equation it defines a *reversible* Markov process that is given by the equation

$$\dot{q} = -\frac{1}{\gamma}\nabla_q V(q) + \frac{\sigma}{\gamma}\dot{W}_t. \tag{2.7}$$

The stochastic differential equation (2.7) defines a continuous time Markov process Q_t on the state space $\mathbf{X} = \Omega$ with invariant probability measure $\mu(\mathrm{d}q) \propto \exp(-\beta V(q))\mathrm{d}q$ [52]. Thus, this dynamical model satisfies our expectation on class (MC2) but should in general not be expected to satisfy those on (MC1). Nevertheless there is a long history of using it as a simple toolkit for investigation of dynamical behavior in complicated energy landscapes [8]. It is known that under weak conditions on the potential function V the Markov process is reversible [35].

Markov Chain Monte Carlo (MCMC). Markov Chain Monte Carlo techniques are designed to sample a given probability density $f : \mathbf{R}^d \to \mathbf{R}$, particularly in highly dimensional state spaces. MCMC is an iterative realization of some specific Markov chain, whose stochastic transition function is given by

$$p(x, \mathrm{d}y) \;=\; q(x, y)\mu(\mathrm{d}y) + r(x)\delta_x(\mathrm{d}y).$$

That is, the stochastic transition function is composed of some transition kernel $q(x, y)$, which is assumed to be μ–integrable and some rejection probability

$$r(x) \;=\; 1 - \int_X q(x, y)\mu(\mathrm{d}y) \;\geq\; 0.$$

In almost all situations, the transition kernel q is chosen in such a way that the stochastic transition function is reversible w.r.t. μ.

In general MCMC is an artificial dynamical model that is in general understood as the embodiment of class (MC2), therefore being in general far from

satisfying the properties of (MC1). However, there are MCMC methods like the popular hybrid Monte Carlo Method (HMC) that can be understood as a special realization of the Hamiltonian system with randomized momenta.

3 Summary

Concerning our main categories (MC1) and (MC2) the summary could be the following: Constant temperature MD, MCMC, the Langevin and Smoluchowski systems clearly belong to (MC2), while the deterministic Hamiltonian system is supposed to be the incorporation of (MC1). However, this distinction is not sharp: the Langevin system is often also accepted as belonging to (MC1), while the deterministic Hamiltonian system is accepted for (MC1) only under the condition that enough details of the entire molecular system (including parts of the solute environment) are represented in atomic resolution and the interaction potential V is appropriate.

Chapter 4. Metastability

Given a dynamical system, metastability of some subset of the state space is characterized by the property that the dynamical system is likely to remain within the subset for a long period of time, until it exits and hence a transition to some other region of the state space occurs. There is no unique but several definitions of metastability in literature (see, e.g., [7, 9, 57, 58]); we will herein focus on two different concepts that are adapted to suit the ensemble dynamics and exit time approach, respectively, as discussed in Section 2.

A subset $C \subset \mathbf{X}$ of the entire state space is called **metastable**, ...

Ensemble Dynamics Approach: ... if the fraction of systems in C, whose trajectory exits during some pre–described time span τ, is significantly small.

Exit Time Approach: ... if with high probability a typical long–term trajectory stays within C longer than some "macroscopic" time span.

Based on the discussion in Section "Conceptual Preliminaries" we would expect to run into trouble when aiming at a "naive" numerical realization of the Exit Time Approach while the Ensemble Dynamics Approach seems to be numerically treatable for short observation time spans τ. We will come back to this question below.

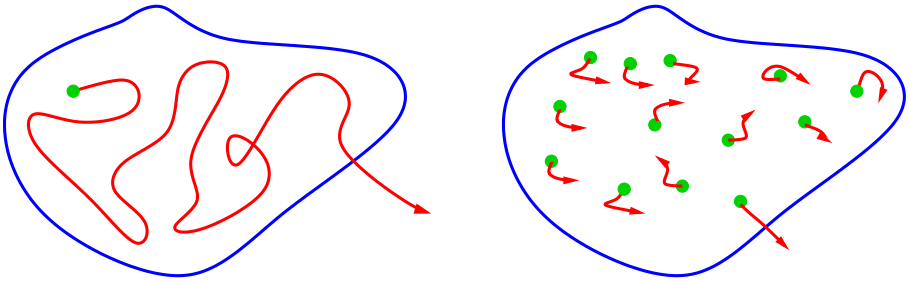

Fig. 4. *Illustration of the different concepts of metastability: Exit Time Approach on the left and Ensemble Dynamics Approach on the right.*

In view of our biochemical application context we aim at the identification of a *decomposition of the state space into metastable subsets* and the corresponding "flipping dynamics" between these. In general, a **decomposition** $\mathcal{D} = \{D_1, \ldots, D_m\}$ of the state space $\mathbf{X}$ is a collection of subsets $D_k \subset \mathbf{X}$ with the properties:

positivity: $\mu(D_k) > 0$ for every k,
disjointness up to null sets: $\mu(D_k \cap D_l) = 0$ for $k \neq l$, and
covering property: $\cup_{k=1}^{m} \overline{D_k} = \mathbf{X}$.

The problem of identifying a decomposition into metastable subsets particularly poses the task of specifying the number m of subsets one is looking for. Within the transfer operator approach this is done via spectral analysis (see *key idea* on page 24).

4 Ensemble Dynamics Approach: Transition Probabilities

We aim at defining an (ensemble) transition probability from a subset B to C within some time span τ, denoted by $p(\tau, B, C)$, such that an invariant sub–ensemble C is characterized by $p(\tau, C, C) = 1$, while a metastable sub–ensemble can be characterized by $p(\tau, C, C) \approx 1$. We will see that within this approach metastability is measured w.r.t. the invariant probability measure μ of the dynamics; in biomolecular systems, the measure μ will often be defined in terms of the canonical ensemble.

We define the **transition probability** $p(t, B, C)$ from $B \subset \mathbf{X}$ to $C \subset \mathbf{X}$ within the time span t as the conditional probability

$$p(t, B, C) \;=\; \mathbf{P}_\mu[X_t \in C \;|X_0 \in B] \;=\; \frac{\mathbf{P}_\mu[X_t \in C \text{ and } X_0 \in B]}{\mathbf{P}_\mu[X_0 \in B]}, \qquad (4.1)$$

where $\mathbf{P}_\mu$ indicates that the initially the Markov process X_t is distributed

according to μ, hence $X_0 \sim \mu$. Exploiting the definition of the stochastic transition function $p(t, x, C)$ in (1.1) we rewrite (4.1) as

$$p(t, B, C) \;=\; \frac{1}{\mu(B)} \int_B p(t, x, C)\, \mu(\mathrm{d}x). \tag{4.2}$$

In other words, the transition probability quantifies the dynamical fluctuations within the stationary ensemble μ. Due to the ensemble dynamics approach to metastability we call a subset $B \subset \mathbf{X}$ **metastable** on the time scale $\tau > 0$ if

$$p(\tau, B, B^c) \approx 0, \quad \text{or equivalently,} \quad p(\tau, B, B) \;\approx\; 1,$$

where $B^c = \mathbf{X} \setminus B$ denotes the complement of B. Obviously, the approximate equalities are not sharp enough for a rigorous definition of metastability. We will come back to this problem in Section 7.

Remark. It is an intrinsic property of the ensemble transition probability to depend on the observation time span τ. It is obvious from its definition that $p(\tau, C, C)$ approaches 1 for $\tau \to 0$, while it decays to $\mu(C)$ for $\tau \to \infty$, see Figure 5. The most interesting phenomena occur on mesoscopic time scales τ. In the biomolecular application context, the observation time span τ will be given by the experimental setting. In the earlier mentioned pump–and–probe experiments, the values of τ range in the sub–picosecond regime.

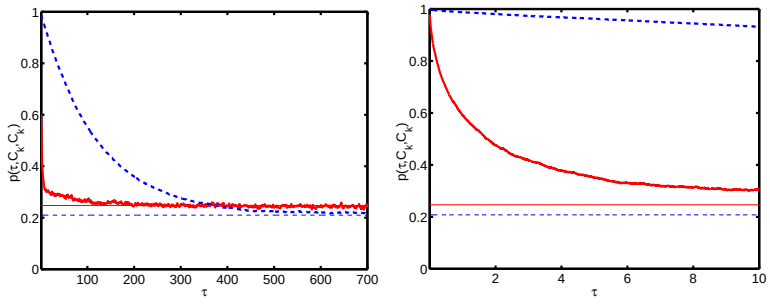

Fig. 5. *Dependence of the transition probability $p(\tau, C, C)$ on the observation time span τ for $0 \le \tau \le 700$ (left) and zoomed into $0 \le \tau \le 10$ (right) w.r.t. two different subsets, one being metastable (dashed line) the other being much less metastable (solid line). The thick line corresponds to $p(\tau, C, C)$, while the corresponding predicted limit value $\mu(C)$ (see text) is indicated by a horizontal thin line. As can be seen from the graphics the distinction between metastable and not–metastable is clearly visible for mesoscopic observation time spans as, e.g., $1/2 \le \tau \le 10$. (The data are based on the Smoluchowski dynamics w.r.t. the perturbed three–well potential as illustrated in Figure 7.)*

5 Exit Time Approach: Exit Rates

The characterization of metastability within the exit time approach is related to the asymptotic decay of the distribution of exit times. Its precise formulation via exit (decay) rates requires some extended mathematical theory that hinders understanding at first reading. Therefore, we prefer to outline the fundamental idea rather than to give its mathematical justification, for which we refer to [37].

Denote by $D \subset \mathbf{X}$ some connected open subset and consider some point $x \in D$. Then the **exit time** $\varrho_D(x)$ of the Markov process X_t from D started at $X_0 = x$ is defined as

$$\varrho_D(x) \;=\; \inf\left\{t \geq 0 : \int_0^t \mathbf{1}_X(X_s \notin D)\,\mathrm{d}s > 0\right\} \tag{5.1}$$

and measures only exits that happen for some non–null time interval neglecting exit events that are "singular" in time. Note that in general ϱ_D is a random variable that depends on the realization of the Markov process X_t.

The fundamental idea is a characterization of metastability in terms of the asymptotic decay of the distribution of exit times

$$F_x(s) \;=\; \mathbf{P}_x[\varrho_D(x) \geq s].$$

While for small values of s the function F_x may show complicated behavior, it asymptotically may decay almost exponentially, at least under certain well–established conditions. The decay rate of F_x can best be expressed by means of the conditional exit time distribution

$$F_x(s,t) \;=\; \mathbf{P}_x[\varrho_D(x) \geq s + t \mid \varrho_D(x) \geq t]$$

for $s, t \geq 0$ that describes the tail of the distribution, for which the exit time is larger than the so–called waiting time t. The decay rate is equal to Γ if the conditional distribution decays exponentially with rate $\Gamma > 0$, i.e.,

$$F_x(s,t) \;\propto\; \exp(-\Gamma s), \tag{5.2}$$

for $s \geq 0$ and $t \geq 0$. When aiming at a definition of metastability in terms of decay rates for entire *subsets*, there are two problems. Firstly, the relation in (5.2) will only hold for very special Markov processes [37]. Secondly, we would expect that the decay rate depends on the starting point, i.e., $\Gamma = \Gamma_x$.

The approach presented herein is based on the fact that there do exist subsets C, for which the decay rate is basically independent for all states $x \in C$. In a more general setting, but for a specific class of dynamical systems including,

e.g., the Smoluchowski dynamics, we are able to assign a so–called **exit rate** $\Gamma = \Gamma(C)$ to an entire subset $C \subset \mathbf{X}$ rather than to single points $x \in \mathbf{X}$, thus circumventing the two above mentioned problems with (5.2). This exit rates may be thought of as some generalization of decay rates; see Appendix B, in particular Theorem B.1.

Due to the exit time approach to metastability we call a subset $B \subset \mathbf{X}$ **metastable** with exit rate $\Gamma(B)$ if

$$\Gamma(A) > \Gamma(B), \quad \text{for all open, connected sets } A \subset B, A \neq B. \tag{5.3}$$

As in the ensemble approach there will be infinitely many metastable subsets and we expect to find a hierarchy of metastability.

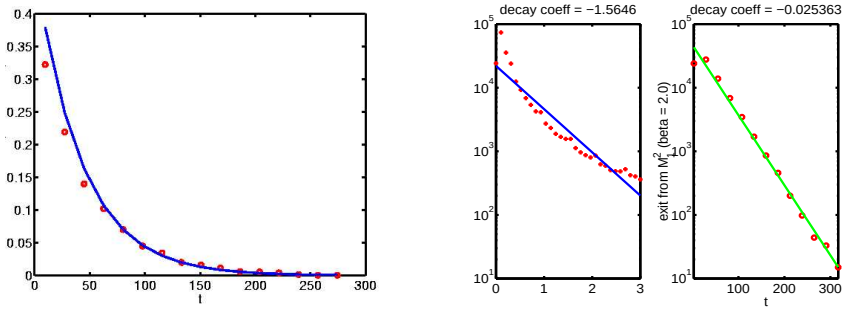

Fig. 6. *Dependence of the exit time distribution $F_x(s)$ on the exit time s for some metastable subset D. The decay is shown for $0 \leq s \leq 300$ (left), and zoomed into $0 \leq s \leq 3$ (middle) and $10 \leq s \leq 300$ (right) on a semi-logarithmic plot. We observe regions of different decay (middle and right). Asymptotically, the decay rate of the exit time distribution is close to the predicted value of $\Gamma(D)$, i.e., $F_x(s)$ for $s > t$ decays approximately with rate $\Gamma(D)$ for $t \to \infty$. Regions of different decay rate (like, e.g., initial rapid decay followed by a much slower decay) are typically due to the fact that with high probability the process exits very rapidly, while with almost vanishing, but existing probability the process moves into some much more metastable region contained in D such that asymptotically the exit rate becomes very small.*

Chapter 5. Transfer Operators

We now give the mathematical foundations and the algorithmic strategies to characterize and identify a decomposition of the state space into metastable subsets. It turns out that in either of the approaches transfer operators and their generators play a crucial role.

6 Transfer Operators and Generators

Based on the assumption that the dynamical description is given by a (homogeneous) Markov process X_t we now introduce a Markov operator that allows to describe the propagation of sub–ensembles in time under the action of X_t. In so doing, we assume in the sequel that the probability measure μ is invariant w.r.t. the Markov process X_t.

The basic idea is the following: Consider all systems within the stationary ensemble μ, whose states are in some subset $C \subset \mathbf{X}$. This sub–ensemble is distributed according to the probability measure

$$\nu_0(A) \;=\; \frac{1}{\mu(C)} \int_A \mathbf{1}_C(x)\mu(\mathrm{d}x) \;=\; \int_A v_0(x)\,\mu(\mathrm{d}x)$$

corresponding to the density $v_0 = \mathbf{1}_C/\mu(C)$ w.r.t. to μ. Since every single microscopic system evolves according to the Markov process defined by its stochastic transition function p, the distribution of the sub–ensemble at time $t \in \mathbf{T}$ is given by the probability measure

$$\nu_t(A) \;=\; \int_{\mathbf{X}} v_0(x)\,p(t,x,A)\;\mu(\mathrm{d}x). \tag{6.1}$$

On the other hand, if ν_t admits the density v_t, we have

$$\nu_t(A) \;=\; \int_A v_t(x)\;\mu(\mathrm{d}x). \tag{6.2}$$

Our interest is to define a transfer operator P^t that propagates sub–ensembles in time according to

$$v_0 \longmapsto v_t = P^t v_0. \tag{6.3}$$

This transfer operator is well–defined due to [35, 51] and acts on the Banach spaces $L^r(\mu)$, $1 \le r \le \infty$ with corresponding norms $\|\cdot\|_r$, as defined in Appendix A. Combining eqs. (6.1) and (6.2), we define the **semigroup of propagators** or forward transfer operators $P^t : L^r(\mu) \to L^r(\mu)$ with $t \in \mathbf{T}$ and $1 \le r < \infty$ as follows:

$$\int_A P^t v(y)\;\mu(\mathrm{d}y) \;=\; \int_{\mathbf{X}} v(x)p(t,x,A)\mu(\mathrm{d}x) \tag{6.4}$$

for $A \subset \mathbf{X}$. As a consequence of the invariance of μ, the characteristic function $\mathbf{1}_{\mathbf{X}}$ of the entire state space is an invariant density of P^t, i.e., $P^t\mathbf{1}_{\mathbf{X}} = \mathbf{1}_{\mathbf{X}}$. Furthermore, P^t is a Markov operator, i.e., P^t conserves norm: $\|P^t v\|_1 = \|v\|_1$ and positivity: $P^t v \ge 0$ if $v \ge 0$, which is a simple consequence of the

definition. Due to (6.3), the semigroup of propagators mathematically models the physical phenomena of evolution of sub–ensembles in time.

In the theory of Markov processes another semigroup of operators is considered. We will call it the **semigroup of backward transfer operators** $T^t : L^r(\mu) \to L^r(\mu)$ with $t \in \mathbf{T}$ and $1 \leq r \leq \infty$, defined by

$$T^t u(x) \;=\; \mathsf{E}_x[u(X_t)] \;=\; \int_{\mathbf{X}} u(y) p(t, x, \mathrm{d}y). \tag{6.5}$$

As a consequence of property (ii) in Appendix A of the stochastic transition function, we have $T^t \mathbf{1}_{\mathbf{X}} = \mathbf{1}_{\mathbf{X}}$ for every $t \in \mathbf{T}$. Both transfer operators are closely related via the duality bracket $\langle v, u \rangle_\mu = \int_{\mathbf{X}} v(x) u(x) \mu(\mathrm{d}x)$ for $v \in L^1(\mu)$ and $u \in L^\infty(\mu)$, namely

$$\langle P^t v, u \rangle_\mu \;=\; \langle v, T^t u \rangle_\mu. \tag{6.6}$$

In discrete time $t \in \mathbf{N}$ it is convenient to use the abbreviations $P = P^1$ and $T = T^1$ corresponding to the stochastic transition function $p(x, \mathrm{d}y) = p(1, x, \mathrm{d}y)$; compare Section 1. Propagators associated with *reversible* Markov processes are of particular interest, since they possess additional structure on the Hilbert space $L^2(\mu)$. Such propagators will be called reversible, too.

Proposition 6.1 ([35]) *Let $P^t : L^2(\mu) \subset L^1(\mu) \to L^2(\mu)$ denote the propagator corresponding to the Markov process X_t. Then P^t is self–adjoint w.r.t. the scalar product $\langle \cdot, \cdot \rangle_\mu$ in $L^2(\mu)$, i.e.,*

$$\langle u, P^t v \rangle_\mu \;=\; \langle P^t u, v \rangle_\mu; \qquad t \in \mathbf{T}$$

for every $u, v \in L^2(\mu)$, if and only if the Markov process X_t is reversible.

For the semigroup of propagators $P^t : L^r(\mu) \to L^r(\mu)$ with $1 \leq r \leq \infty$ define $\mathcal{D}(\mathcal{A})$ as the set of all $v \in L^r(\mu)$ such that the strong limit

$$\mathcal{A} v \;=\; \lim_{t \to \infty} \frac{P^t v - v}{t}$$

exists. Then, the operator $\mathcal{A} : \mathcal{D}(\mathcal{A}) \to L^r(\mu)$ is called the infinitesimal **generator** corresponding to the semigroup P^t [40, 43].

Remark. Physical experiments on molecular ensembles allow to measure relative frequencies in the canonical ensemble μ. Suppose again that μ has the form

$$\mu(\mathrm{d}x) \;=\; f(x) \mathrm{d}x,$$

i.e., μ is absolutely continuous w.r.t. the Lebesgue measure $\mathrm{d}x$. Then physical experiments are related to densities of the form

$$v_{\mathrm{phys}}(x) \;=\; \hat{\mathbf{1}}_C(x) f(x) \in L^1(\mathrm{d}x)$$

w.r.t. the Lebesgue measure $\mathrm{d}x$. Whenever physicists use the phrase "probability density" they refer to v_{phys} rather than to densities

$$v_{\mathrm{math}}(x) \;=\; \hat{\mathbf{1}}_C(x) \in L^1(\mu)$$

w.r.t. probability measure μ, as we do. As it will become apparent later, it is mathematically advantageous to consider the semigroup of propagators acting on densities v_{math} rather than the semigroup of propagators acting on v_{phys}. In the former approach, we have $P^t \mathbf{1}_{\mathbf{X}} = \mathbf{1}_{\mathbf{X}}$, while in the latter this would read $P^t f = f$. However, it should be clear that results obtained in either of the two descriptions can be transformed into the other.

Examples. To be more specific, we now list the propagators for the different dynamical descriptions introduced in Section 2.

The propagator corresponding to the deterministic Hamiltonian system with flow Φ^t is known as the Frobenius–Perron operator [43] given by

$$P^t u(x) = u(\Phi^{-t} x).$$

For the Hamiltonian system with randomized momenta we have a kind of Frobenius–Perron operator averaged w.r.t. the momenta,

$$P^t u(q) \;=\; \int_{\mathbf{R}^d} u(\Pi_q \Phi^{-\tau}(q,\xi)) \mathcal{P}(\xi) \mathrm{d}\xi. \tag{6.7}$$

For MCMC the propagator is given by

$$Pu(y) = \int q(x,y) u(x)\, \mathrm{d}x + r(y) u(y). \tag{6.8}$$

For Langevin and Smoluchowski dynamics, the semigroups of propagators admit strong generators $\mathcal{A}_{\mathrm{Smo}}$ and $\mathcal{A}_{\mathrm{Lan}}$ in $L^r(\mu)$ for $1 \le r < \infty$ such that the semigroups can be written as

$$P^t_{\mathrm{Smo}} \;=\; \exp(t\mathcal{A}_{\mathrm{Smo}}) \quad \text{and} \quad P^t_{\mathrm{Lan}} \;=\; \exp(t\mathcal{A}_{\mathrm{Lan}}),$$

respectively. For twice continuously differentiable $u \in L^r(\mu)$ we have the identity

$$\mathcal{A}_{\mathrm{Smo}}\, u \;=\; \left(\frac{\sigma^2}{2\gamma^2} \Delta_q - \frac{1}{\gamma} \nabla_q V(q) \cdot \nabla_q \right) u$$

$$\mathcal{A}_{\mathrm{Lan}}\, u \;=\; \left(\frac{\sigma^2}{2}\Delta_p \;-\; p\cdot\nabla_q \;+\; \nabla_q V\cdot\nabla_p \;-\; \gamma p\cdot\nabla_p\right) u.$$

For details on $\mathcal{A}_{\mathrm{Smo}}$ and $\mathcal{A}_{\mathrm{Lan}}$ see the theory of Fokker-Planck equations and Kolmogoroff forward and backward equations [52, 57, 35].

7 Detecting Metastability

The key idea of the transfer operator approach to metastability is to exploit the strong relation between stability properties of the Markov process and the presence of special eigenvalues in the spectrum.

Since propagators are Markov operators by definition, their spectrum is contained in the unit circle of the complex plane, i.e., the modulus of every eigenvalue is smaller or equal to 1. Suppose that some proper subset $C \subset \mathbf{X}$ is invariant under the Markov process, i.e., $p(t, x, C^c) = 0$ for all $x \in C$. Then we have:

> *ensemble dynamics approach*: the transition probability from C into its complement C^c is zero: $p(t, C, C^c) = 0$ for *every* $t \in \mathbf{T}$,
>
> *exit rate approach*: the exit rate from C is zero: $\Gamma(C) = 0$.

In literature on Markov and transfer operators, it is a well–known fact that the existence of invariant subsets has spectral consequences. Under well–established stability conditions (see (C1) and (C2) on page 24), we have:

> *transfer operator*: the propagator P^t exhibits an eigenvalue $\lambda_t \equiv 1$ with corresponding eigenfunction $\mathbf{1}_C$, hence $P^t\mathbf{1}_C = \mathbf{1}_C$ for every $t \in \mathbf{T}$.

Now suppose that the entire state space decomposes into exactly two invariant subsets, $X = B \cup C$. Then, according to (iii) the eigenvalue $\lambda = 1$ is two–fold, one corresponding to each invariant subset associated with the eigenfunctions $\mathbf{1}_B$ and $\mathbf{1}_C$. Introducing a weak coupling between the subsets B and C yields one invariant set, namely the entire state space $\mathbf{X}$, and two *weakly coupled* or *metastable* subsets, namely B and C. This has the following consequences:

> *ensemble dynamics approach*: the transition probability from B to C is almost zero: $p(\tau, B, C) \approx 0$ for $0 < \tau < T$ with large T. The same holds for the transition probability from C to B.

exit rate approach: the exit rates from B and C are very small: $\Gamma(B) \approx 0$ and $\Gamma(C) \approx 0$.

transfer operator: for $0 < \tau < T$ with large T, the propagator P^τ exhibits two dominant eigenvalues. More precisely, there exists $\eta_t \equiv 1$ corresponding to the invariant state space, and one eigenvalue $\lambda_\tau \approx 1$ corresponding to the weak coupling between the subsets B and C.

To the end, we fix some $\tau > 0$ and abbreviate $P = P^\tau$ and $p(x, C) = p(\tau, x, C)$. Hence, $(P)^n = P^{n\tau}$ corresponds to the Markov process sampled at rate τ with stochastic transition function given by $p^n(\cdot, \cdot) = p(n\tau, \cdot, \cdot)$.

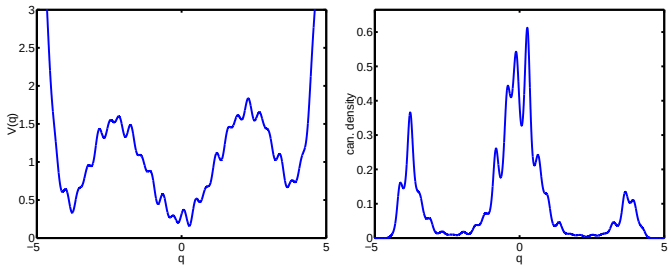

Fig. 7. *Left: a perturbed three well potential V used for illustration. Right: canonical density corresponding to $\beta = 3.0$. Assume that the internal dynamics is given by the Smoluchowski system corresponding to $\gamma = 2.0$ and σ given by eq. (2.6). The dominant spectrum of the propagator $P = P^\tau$ with $\tau = 1.0$ exhibits three eigenvalues close to 1. More precisely, we have $\lambda_1 = 1.0000$, $\lambda_2 = 0.9924$, $\lambda_3 = 0.9886$, which are separated from the remaining eigenvalues by a significant gap, since $\lambda_4 = 0.6634$. According to the key idea of the transfer operator approach we expect a decomposition of the state space into three metastable subsets, which is in agreement with our intuition for the above potential.*

The above considerations motivate the following **key idea of the transfer operator approach**:

Metastable subsets can be detected via eigenvalues of the propagator P close to its maximal eigenvalue $\lambda = 1$; moreover they can be identified by exploiting the corresponding eigenfunctions. In doing so, the number of metastable subsets is equal to the number of eigenvalues close to 1, including $\lambda = 1$ and counting multiplicity.

The strategy mentioned above has first been proposed by Dellnitz and Junge [11] for discrete dynamical systems with weak random perturbations and has been successfully applied to molecular dynamics in different contexts [55, 56, 54]; its justification is given in Section 9. The key idea requires the following two **conditions on the propagator** P (for a definition of the essential spectral radius see Appendix A):

(C1) The essential spectral radius of P is less than one, i.e., $r_{\text{ess}}(P) < 1$.

(C2) The eigenvalue $\lambda = 1$ of P is simple and dominant, i.e., $\eta \in \sigma(P)$ with $|\eta| = 1$ implies $\eta = 1$.

While condition (C1) allows to ensure convergence results of the numerical discretization scheme, condition (C2) excludes modeling and interpretation problems; for more details see [54, 35]. In order to proceed along the way indicated by the key idea we have to check in which situations the two conditions (C1) and (C2) may hold. In this section, we establish sufficient conditions on the Markov process that imply (C1) and (C2). Here, we mainly concentrate on reversible propagators P on $L^2(\mu)$ and refer for $L^1(\mu)$ and L^∞_V to [35] and [48], respectively.

There are some sufficient conditions to guarantee the spectral properties of the propagator that are related to well studied stability properties of Markov processes. The $\mathcal{V}$–norm and total variation norm $\|\cdot\|_{\mathrm{TV}}$ stated in the next definition are defined in Appendix A:

Definition 7.1 *Let p denote some stochastic transition function. Then*

*(a) p is called **geometrically ergodic** if*

$$\|p^n(x,\cdot) - \mu\|_{\mathrm{TV}} \;\leq\; \mathcal{V}(x)q^n; \qquad n \in \mathbf{N} \tag{7.1}$$

for every $x \in \mathbf{X}$, some constant $q < 1$, and some integrable function $\mathcal{V} : \mathbf{X} \to \mathbf{R}$ satisfying $\mathcal{V} < \infty$ pointwise.

*(b) p is called $\mathcal{V}$–**uniformly ergodic** if*

$$\|p^n(x,\cdot) - \mu\|_{\mathcal{V}} \;\leq\; C\mathcal{V}(x)q^n; \qquad n \in \mathbf{N}$$

for every $x \in \mathbf{X}$, constants $q < 1$ and $C \leq \infty$, and some function $\mathcal{V} \in L^1(\mu)$ satisfying $1 \leq \mathcal{V}$ pointwise.

The relation between geometrical and $\mathcal{V}$–uniform ergodicity is as follows: By definition, V–uniform ergodicity implies geometric ergodicity. On the other hand, for irreducible and aperiodic stochastic transition functions geometric ergodicity implies V–uniform ergodicity according to [53, Proposition 2.1]. Either form of ergodicity implies the properties of interest:

Theorem 7.2 ([35]) *Let $P : L^2(\mu) \to L^2(\mu)$ denote a reversible propagator. Then P satisfies conditions (C1) and (C2) in $L^2(\mu)$, if its stochastic transition function is geometrically or $\mathcal{V}$–uniformly ergodic.*

Conditions, under which Markov processes are geometrically or $\mathcal{V}$–uniformly ergodic are widely studied; for sufficient conditions w.r.t. the dynamical models introduced in Section 3 see, e.g., [35, Sec. 6] and cited references, or [47, 54].

8 Identification Algorithm

The key idea of the transfer operator approach needs to be specified regarding the actual *algorithmic identification* of metastable subsets based on the most dominant eigenvectors. The basic idea is to reduce the problem of identifying a decomposition into metastable subsets to a clustering problem, which is done by incorporating dynamical information into the process of clustering. It is therefore different from statistical clustering that is solely based on geometrical information.

Following the key idea of the transfer operator approach we are aiming at a decomposition $\mathcal{D} = \{D_1, \ldots, D_m\}$ of the state space into m metastable subsets $D_1, \ldots, D_m$ such that the number of subsets m equals the number of dominant eigenvalues. Figure 8 demonstrates the mechanism of the transfer operator approach to metastability.

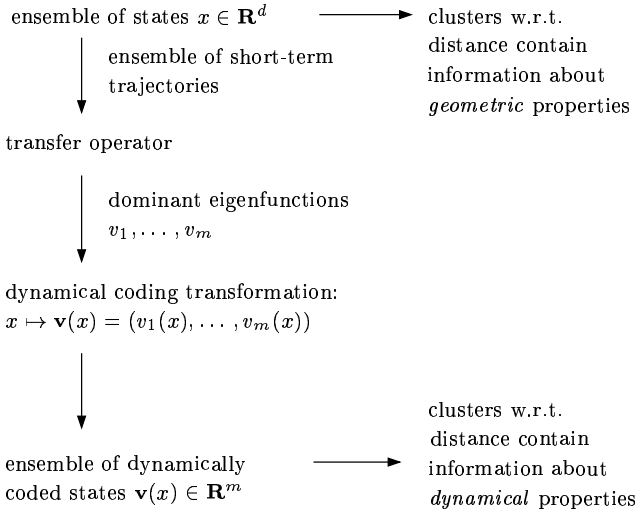

Fig. 8. *Basic mechanism of incorporating dynamical information via dominant eigenfunctions of the transfer operator. Note that the dimension of the state space that have to be clustered reduces from d to m. In biomolecular applications, typically we have* $m \ll d$.

Based on this mechanism, virtually almost every cluster algorithm can be used to identify a decomposition of the state space into metastable subsets, *if applied to the dynamically coded sampling points.* The identification procedure introduced in [17] computes this decomposition from the *sign structure* of the coded sampling points as illustrated in Figure 10. Given the m dominant eigenvectors $v_1, \ldots, v_m$, we can assign to every state $x \in \mathbf{X}$ a unique *sign structure*

$$s(x) = \Big(s_1(x), \ldots, s_m(x)\Big) = \{+, -\}^m,$$

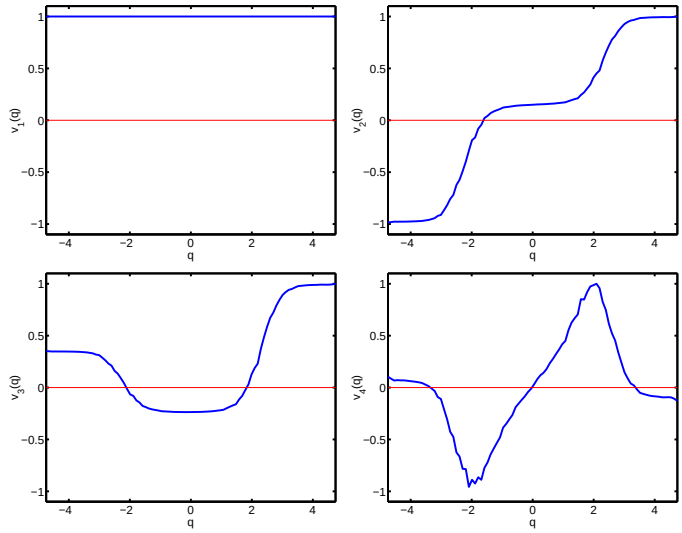

Fig. 9. *Eigenfunction corresponding to propagator based on the Smoluchowski system in application to the perturbed three well potential V as illustrated in Figure 7. Eigenfunctions corresponding to the largest eigenvalues* $1.0000, 0.9924, 0.9886, 0.6634$ *(clockwise, starting top–right). As expected, the eigenfunction corresponding to* $\lambda_1 = 1$ *is constant. Note that the second and the third eigenfunction exhibit a very special structure: they are almost constant around the three wells (cf. potential in Fig. 7), while they show jumps near the saddle point regions.*

where for some prescribed threshold value θ we define the "unambiguous" positive or negative sign $s_k(x)$ of $v_k(x)$ as

$$s_k(x) \;=\; \begin{cases} +\,;\; v_k(x) > \theta \\ -\,;\; v_k(x) < \theta \end{cases}$$

as explained in Figure 10. Denote by $S(\mathbf{X}) \subset \mathbf{X}$ the set of all states with at least one "unambiguous" sign s_k. If θ is large enough and the eigenfunctions are smooth, $S(\mathbf{X})$ decomposes into exactly m subsets each containing states of the same sign structure only [17]. These are the "core sets" of the metastable subsets. States with "unambiguous" sign structure are assigned to these core sets [17] such that the resulting m metastable sets decompose the state space. This clustering algorithm has proved to be successful in many different situations; in the following subsection we give a mathematical justification of the algorithmic identification strategy from the point of view of the ensemble dynamics and the exit time approach.

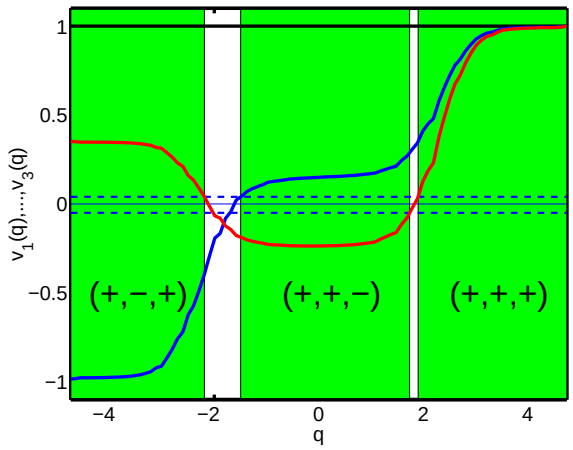

Fig. 10. *Illustration of the identification procedure based on the perturbed three well potential presented in Figure 7. The three grey shaded regions indicate the parts of the q-axis on which the three most dominant eigenvectors exhibit "unambiguous" sign structures (here* $\theta = 0.05$ *as indicated by dashed lines). To give an example: the grey shaded region on the very left has sign structure* $(+,-,+)$ *since* $v_1(q), v_3(q) > \theta$ *and* $v_2(q) < -\theta$ *for all states* q *on the very left.*

9 Mathematical Justification

We now give a mathematical justification of the key idea of the transfer operator approach, which illuminates the strong relation between the existence of a cluster of eigenvalues close to 1 and a possible decomposition of the state space into metastable subsets.

Justification within the Ensemble Dynamics Approach. The investigation will be based on the following assumptions: The propagator $P : L^2(\mu) \to L^2(\mu)$ satisfies conditions (C1), (C2) and the underlying Markov process is reversible. As a consequence the propagator P is self–adjoint due to Proposition 6.1.

The close relation between transition probabilities and transfer operators becomes transparent in

$$p(B,C) \;=\; \frac{\langle P\mathbf{1}_B, \mathbf{1}_C\rangle_\mu}{\langle \mathbf{1}_B, \mathbf{1}_B\rangle_\mu} \;=\; \frac{\langle \mathbf{1}_B, T\mathbf{1}_C\rangle_\mu}{\langle \mathbf{1}_B, \mathbf{1}_B\rangle_\mu}. \tag{9.1}$$

Eq. 9.1 allows to give a mathematical statement relating dominant eigenvalues, the corresponding eigenfunctions and a decomposition of the state space into metastable subsets. For later reference we define the **metastability of a decomposition** $\mathcal{D}$ as the sum of the metastabilities of its subsets. The next result can be found in [38]; a version for two subsets was published in [35].

Theorem 9.1 *Let $P : L^2(\mu) \to L^2(\mu)$ denote a reversible propagator satisfying (C1) and (C2). Then P is self–adjoint and the spectrum has the form*

$$\sigma(P) \subset [a, b] \cup \{\lambda_m\} \cup \ldots \cup \{\lambda_2\} \cup \{1\}$$

with $-1 < a \leq b < \lambda_m \leq \ldots \leq \lambda_1 = 1$ and isolated, not necessarily simple eigenvalues of finite multiplicity that are counted according to multiplicity. Denote by $v_m, \ldots, v_1$ the corresponding eigenfunctions, normalized to $\|v_k\|_2 = 1$. Let Q be the orthogonal projection of $L^2(\mu)$ onto $\mathrm{span}\{\mathbf{1}_{A_1}, \ldots, \mathbf{1}_{A_m}\}$. The metastability of an arbitrary decomposition $\mathcal{D} = \{A_1, \ldots, A_m\}$ of the state space $\mathbf{X}$ can be bounded from above by

$$p(A_1, A_1) + \ldots + p(A_m, A_m) \leq 1 + \lambda_2 + \ldots + \lambda_m,$$

while it is bounded from below according to

$$1 + \kappa_2\lambda_2 + \ldots + \kappa_m\lambda_m + c \leq p(A_1, A_1) + \ldots + p(A_m, A_m)$$

where $\kappa_j = \|Qv_j\|^2_{L^2(\mu)}$ and $c = a\,(1 - \kappa_2) \ldots (1 - \kappa_n)$.

Theorem 9.1 highlights the strong relation between a decomposition of the state space into metastable subsets and dominant eigenvalues close to 1. It states that the metastability of an arbitrary decomposition $\mathcal{D}$ cannot be larger than $1 + \lambda_2 + \ldots + \lambda_m$, while it is at least $1 + \kappa_2\lambda_2 + \ldots + \kappa_m\lambda_m + c$, which is close to the upper bound whenever the dominant eigenfunctions $v_2, \ldots, v_m$ are almost constant on the metastable subsets $A_1, \ldots, A_m$ implying $\kappa_j \approx 1$ and $c \approx 0$. The term c can be interpreted as a correction that is small, whenever $a \approx 0$ or $\kappa_j \approx 1$. It is demonstrated in [38] that the lower and upper bounds are sharp and asymptotically exact.

In view of Theorem 9.1, it is natural to ask, whether there is an *optimal* decomposition with highest possible metastability. The answer is illustrated by Figure 11: *Even if there exists an optimal decomposition, the problem of finding it might be ill–conditioned.* The graph shows the metastability of a family of decompositions. It is based on the propagator P corresponding to the Smoluchowski dynamics for the perturbed three–well potential. We identify a flat plateau of decompositions that are nearly optimal. In this case the problem of finding the maximum is ill–conditioned. We also observe that the decomposition suggested by our identification algorithm is nearly optimal. The phenomenon illustrated by Figure 11 is believed to be typical in our application context, which is due to the fact that the state space admits large regions corresponding to almost vanishing statistical weight (see also [38]).

Justification within the Exit Time Approach. The justification has been worked out in [37] based on recent literature on Markov chains. The most important restriction of this approach is the restriction to Markov processes with

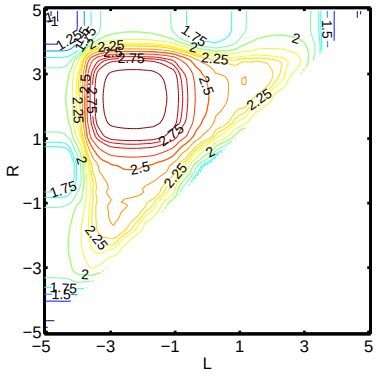

Fig. 11. *Metastability of the decomposition of the state space* $\mathbf{X} = \mathbf{R}$ *into three subsets* $\mathcal{D} = \{A, B, C\}$ *with* $A = (-\infty, L)$, $B = [L, R)$ *and* $C = [R, \infty)$ *parameterized by* $L < R \in \mathbf{R}$. *The problem of finding the maximal value corresponding to the optimal decomposition is often ill–conditioned. There is a large region roughly characterized by* $-3 < L < -1$ *and* $1 < R < 3$, *in which the metastability of the corresponding decomposition is almost maximal. This region is more or less a flat plateau, for which the absolute maximum is hard to identify. The identification algorithm based on the sign structure identifies a decomposition with* $L = -2.13$ *and* $R = 1.84$ *with corresponding metastability* 2.9558, *which is quite close to the upper bound of* 2.9916 *resulting from Theorem 9.1. (Data based on Smoluchowski dynamics as illustrated in Figure 7.)*

continuous sample paths that admit a generator.

We will herein formulate the result for general Smoluchowski systems of type (2.7) from Section 2, because this allows us to remain within the framework of self-adjoint propagators with real-valued eigenvalues and eigenfunctions. The generalization to Langevin systems seems to be possible but requires immense technical effort.

Theorem 9.2 *Assume that there is some continuous Lyapunov function* $\mathcal{V}$ *such that the Markov process is* $\mathcal{V}$*–uniformly ergodic, and that there exists a twice continuously differentiable eigenfunction* $v \colon \mathbf{X} \to \mathbf{R}$ *of the Smoluchowski generator* $\mathcal{A} = \mathcal{A}_{Smo}$. *Hence, there exists some eigenvalue* $\Lambda < 0$ *such that*

$$\mathcal{A}\, v \;=\; \Lambda\, v. \tag{9.2}$$

Suppose moreover that the set C *under consideration and the eigenfunction* h *satisfy the following conditions:*

(1) $v(x) > 0$ *or* $v(x) < 0$ *for all* $x \in C$,
(2) $v(x) = 0$ *and* $(\nabla v(x))^T (\nabla v(x)) > 0$ *for* $x \in \partial C$.
(3) $K_n = \{x \in \mathbf{X} : \mathcal{V}(x) \leq n v(x)\}$ *is a compact subset of* $\mathbf{X}$ *for all* $n \geq 1$.

Then, the set C *is metastable in the sense of definition (5.3) with exit rate*

$\Gamma(C) = -\Lambda$, *where* Λ *is the eigenvalue associated with* v.

This theorem has the following intriguing interpretation: If there is an eigenvalue $-\Gamma_0$ of the generator close to zero, then there is an eigenvalue $\exp(-\tau\Gamma_0)$ of the propagator P^τ close to $\lambda = 1$. The corresponding eigenfunction v of the generator is also the eigenfunction of the propagator. The set of zeros of this eigenfunction decomposes the state space into *open, connected subsets* C_k, restricted to each of which the eigenfunction is either positive or negative. Now Theorem 9.2 states that each of this subsets C_k is metastable with the same rate $\Gamma(C_k) = \Gamma_0$ which is considerably small since Γ_0 is.

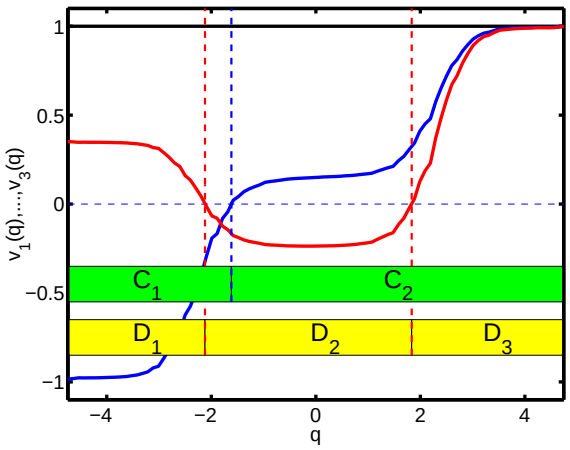

Fig. 12. *Illustration of Theorem 9.2 for the perturbed three well potential illustrated in Figure 7. The lowest eigenfunctions of the generator corresponding to the Smoluchowski dynamics are* $\Lambda_1 = 0.0000$, $\Lambda_2 = -0.0076$, $\Lambda_3 = -0.0114$, *while* $\Lambda_4 = -0.4104$. *The eigenfunctions* v_2 *and* v_3 *exhibit sign changes and allow to decompose the state space into subsets, on which the eigenfunction is either positive or negative. Since* v_2 *has exactly one zero a thereon based decomposition of the state space yields the subsets* C_1 *and* C_2 *with common exit rate* $\Gamma_2 = -\Lambda_2 = 0.0076$. *Analogously,* v_3 *defines the subsets* D_1, D_2 *and* D_3 *with common exit rate* $\Gamma_3 = -\Lambda_3 = 0.0114$.

The identification algorithm is based on the *collection* of the most dominant eigenfunctions. In seemingly contrast, Theorem 9.2 indicates that *each* single eigenfunction induces a metastable decomposition, in particular that different eigenfunctions might induce different metastable decompositions. We illustrate this for the three–well potential in Figure 12. The second and third eigenfunctions v_2 and v_3 allow application of Theorem 9.2 and induce two different decompositions, namely $\{C_1, C_2\}$ and $\{D_1, D_2, D_3\}$. The rate of metastability of the first is superior ($\Gamma(C_k) = 0.022$); the latter reproduces the three-well structure of the potential but its metastable subsets show less significant metastability ($\Gamma(D_k) = 0.036$). Conclusively, the result is a hierarchy of metastable decompositions with decreasingly significant metastability of the subset. However, the identification algorithm will result in a very similar hierarchy if iteratively applied to the set $\{v_1, v_2\}$ of eigenfunctions first and then

to the set $\{v_1, v_2, v_3\}$.

Chapter 6. Numerical Realization

Identification of metastable subsets necessitates the computation of the most dominant eigenfunctions of the propagator $P = P^\tau$ for some fixed observation time span $\tau > 0$. In the following we describe the discretization procedure of the eigenvalue problem $Pv = \lambda v$. Throughout this section we assume that P satisfies the conditions (C1) and (C2) defined in Section 7. Part of this section follows from [54, 55].

10 Galerkin Discretization

Let $\chi = \{\chi_1, \ldots, \chi_n\} \subset L^2(\mu)$ denote a set of *non–negative* functions with the property to yield a partition of unity, i.e.,

$$\sum_{k=1}^{n} \chi_k \;=\; \mathbf{1_X}.$$

The **Galerkin projection** $\Pi_n : L^2(\mu) \to \mathcal{S}_n$ onto the associated finite dimensional ansatz space $\mathcal{S}_n = \text{span}\{\chi_1, \ldots, \chi_n\}$ is defined by

$$\Pi_n v \;=\; \sum_{k=1}^{n} \frac{\langle v, \chi_k \rangle_\mu}{\langle \chi_k, \chi_k \rangle_\mu} \chi_k.$$

Application of the Galerkin projection to $Pv = \lambda v$ yields an eigenvalue problem for the discretized propagator $\Pi_n P \Pi_n$ acting on the finite-dimensional space $\mathcal{S}_n$. The matrix representation of this finite dimensional operator is given by the $n \times n$ *transition matrix* $S = (S_{kl})$, whose entries are given by

$$S_{kl} \;=\; \frac{\langle P\chi_k, \chi_l \rangle_\mu}{\langle \chi_k, \chi_k \rangle_\mu} \;=\; \frac{\langle \chi_k, T\chi_l \rangle_\mu}{\langle \chi_k, \chi_k \rangle_\mu}, \tag{10.1}$$

where T denotes the adjoint transfer operator.

Properties of discretization matrix. Since P is a Markov operator and χ a partition of unity, the Galerkin discretization S is a (row) stochastic matrix, i.e., $S_{kl} \geq 0$ and $\sum_{l=1}^{n} S_{kl} = 1$ for $k = 1, \ldots, n$. Consequently, all its eigenvalues λ satisfy $|\lambda| \leq 1$. Moreover, we have the following three important properties [54, 55]:

(1) The row vector $\pi = (\pi_1, \ldots, \pi_n)$ with $\pi_k = \langle \chi_k, \chi_k \rangle_\mu = \|\chi_k\|_\mu^2$ represents the discretized invariant probability measure μ. It is a left eigenvector corresponding to the eigenvalue $\lambda = 1$, thus $\pi S = \pi$.

(2) S is *irreducible* and *aperiodic*. As a consequence, the eigenvalue $\lambda = 1$ is *simple* and *dominant*, hence $\lambda \in \sigma(S)$ implies $\lambda = 1$ or $|lambda| < 1$. In particular, the discretized invariant density π is the *unique* invariant density of S.

(3) If P is reversible then S is *self–adjoint* w.r.t. the discrete scalar product $\langle u, v\rangle_\pi = \sum u_i \bar{v}_i \pi_i$. Equivalently, S satisfies the *detailed balance condition* $\pi_k S_{kl} = \pi_l S_{lk}$ for every $k, l \in \{1, \ldots, n\}$. Hence, all eigenvalues of S are real–valued and contained in the interval $(-1, 1]$.

Partitions of unity that are defined in terms of some decomposition $\mathcal{D} = \{D_1, \ldots, D_n\}$ of the state space are of particular interest. Any decomposition $\mathcal{D}$ defines a partition of unity $\chi = \{\chi_1, \ldots, \chi_n\}$ with $\chi_k = \mathbf{1}_{D_k}$. Galerkin discretization based on this *box discretization* then yields a transition matrix that in addition to the above properties has the advantageous property that its entries are one–step transition probabilities from D_k to D_l

$$S_{kl} \;=\; \frac{\langle P\mathbf{1}_{D_k}, \mathbf{1}_{D_l}\rangle_\mu}{\langle \mathbf{1}_{D_k}, \mathbf{1}_{D_k}\rangle_\mu} \;=\; p(D_k, D_l).$$

Another prominent example is given by partitions of unity χ whose elements $\chi_k \in \chi$ are so-called mollifies, i.e., non-negative C^∞-functions of compact support that approximate indicator functions. In this case, the discretization often is called *fuzzy set discretization*.

Summarizing, the discretization of the propagator can be interpreted as a *coarse graining* procedure, especially in the case of box discretization: Coarse graining the state space $\{x \in \mathbf{X}\} \to \{D_1, \ldots, D_n\}$ results in a coarse graining of the propagator $P \to S$ corresponding to a coarse graining of the Markov process $p(x, D) \to p(D_k, D_l)$ with invariant measures $\mu \to \pi$. In doing so, the discretization inherits the most important properties of the propagator.

Remark. It is important to notice that—unless in very special situations—the discretization process does not commute with the semigroup property of the transfer operator P. Hence, in general we have

$$(S^2)_{kl} \;\neq\; p^2(D_k, D_l),$$

where S^2 denotes the square of the transition matrix S obtained from discretization P, and p^2 denotes the stochastic transition function corresponding to P^2.

11 The Eigenvalue Problem

We restrict our considerations to the important class of *reversible* propagators $P : L^2(\mu) \to L^2(\mu)$ satisfying the conditions (C1) and (C2).

Under these assumptions, convergence results for the eigenvalues are simple consequences of, e.g., the Rayleigh-Ritz theory (see [54] for details). Obviously we have to require that the sequence of the Galerkin ansatz spaces $\mathcal{S}_{n_1} \subset \mathcal{S}_{n_2} \subset \ldots$ is dense in $L^2(\mu)$, and the corresponding partitions of unity $\chi^{(1)}, \chi^{(2)}, \ldots$ are getting gradually finer, e.g., $\max_{\Phi \in \chi^{(k)}} \mathrm{diam}(\mathrm{supp}\ \Phi) \to 0$ as $n_k \to \infty$ with $k \to \infty$, where we assume that the functions in the kth partition of unity $\chi^{(k)}$ have compact support.

For the explicit numerical approximation of the dominant eigenvalues and eigenvectors different settings are available. Whenever one is interested in the dominant eigenvalues and eigenvectors of the transition matrix for a given discretization one may use iterative eigenvalue solvers, see, e.g., [45]. These allow to compute the desired information even for matrices of size $10^6 \times 10^6$, for example. Whenever one is interested in subsequent refinements of the discretization to achieve approximations with high precision, one should apply multigrid techniques with optimal efficiency even for very fine grids like those constructed in [14], for example. The mentioned preconditions for efficient convergence of the techniques perfectly fit to the scenario of metastability: it is required that the dominant eigenvalues are separated from the remainder of the spectrum by a significant gap. Then the convergence rate of those methods only depends on the spectral gap and is in principle independent of the size of the stochastic transition matrix. The numerical effort is given mainly by the effort of matrix-vector multiplications.

We emphasize, however, that already for small molecules the dimension of state space X is so high as to make the transfer operator approach computationally infeasible if naively applied directly in X. This problem is sometimes called the *curse of dimensionality*. To some extend it can be ameliorated by the use of adaptive algorithms such as those in [10] but, for many problems in high dimensions, combination of the transfer operator approach with clustering approaches, and/or with mathematical modeling such as the exploitation of fast/slow time-scale separation, is needed to circumvent the curse of dimensionality. We will address this problem in Section 14.

12 Evaluation of Transition Matrix

We consider the evaluation of the stochastic transition matrix S obtained from discretizing $P = P^\tau$. The corresponding discrete time Markov chain is denoted by $X_n = \{X_n\}_{n\in\mathbf{N}}$. Consider two elements χ_k, χ_l of the partition of unity used for discretization. Combining $T^\tau\chi_l(x) = \mathsf{E}_x[\chi_l(X_\tau)]$ with (10.1) yields

$$S_{kl} \;=\; \frac{1}{\langle\chi_k,\chi_k\rangle_\mu}\int_{\mathbf{X}} \chi_k(x)\mathsf{E}_x[\chi_l(X_\tau)]\,\mu(\mathrm{d}x),$$

which can be approximated within two steps:

(A1) approximation of the integral

$$\int_B g(x)\,\mu(\mathrm{d}x) \;\approx\; \sum_{k=1}^{N}\alpha_k\,g(x_k)$$

by some deterministic or stochastic integration scheme with partition points or random variables $x_1,\ldots,x_N$, respectively, and weights $\alpha_1,\ldots,\alpha_N$ [16, 31];

(A2) approximation of the expectation value

$$\mathsf{E}_x[\chi_l(X_\tau)] \;\approx\; \frac{1}{M}\sum_{j=1}^{M}\chi_l\left(X_\tau(\omega_j,x)\right)$$

by relative frequencies, where $X_\tau(\omega_k,x)$ denotes a realization of the Markov process with initial distribution $X_0 = x$ [48, Chapter 17].

A combination of (A1) and (A2) with $g(x) = \chi_k(x)\mathsf{E}_x[\chi_l(X_\tau)]$ results in

$$S_{kl} \;\approx\; \frac{1}{M}\sum_{k=1}^{N}\sum_{j=1}^{M}\alpha_k\,\chi_k(x)\cdot\chi_l\left(X_\tau(\omega_{kj},x_k)\right);$$

hence, for each initial point x_k, the Markov process X_τ is realized M times. The approximation quality depends on the interplay between the two approximation steps (A1) and (A2). Numerical experiments in low dimensions show that it is even possible to choose small M, if the number of partition points N is chosen in such a way that the number of points in the support of any of the χ_k is reasonably large. For high–dimensional problems, we will in general be forced to use stochastic integration schemes such as Monte Carlo methods in order to approximate the integral in (A1). For the analysis of biomolecules Monte Carlo based techniques have been applied successfully [55, 36].

Whenever the discrete time Markov process $X_n = \{X_n\}_{n\in\mathbf{N}}$ is ergodic w.r.t. μ, and a statistically representative realization of X_n is available, we may also combine (A1) and (A2):

Example 12.1 *Let $x_0, \ldots, x_N$ denote a sequence of sampling points obtained from a realization of the discrete time Markov process X_n. Then*

$$S_{kl} \approx S_{kl}^{(N)} = \frac{\sum_{j=1}^{N} \chi_k(x_j) \cdot \chi_l(x_{j+1})}{\sum_{j=1}^{N} \chi_k(x_j)^2}, \tag{12.1}$$

where convergence is guaranteed for μ–a.e. initial points x_0 by conditions (C1) and (C2) and the law of large numbers [48].

13 Trapping Problem

The *rate of convergence* of $S_{kl}^{(N)} \to S_{kl}$ depends on the smoothness of the partition functions χ_k as well as on the mixing properties of the Markov chain X_n [46]. The latter property is crucial here: The convergence is geometric with a rate constant $\lambda_1 - \lambda_2 = 1 - \lambda_2$ where λ_2 denotes the second largest eigenvalue (in modulus). That is, in case of metastability and thus λ_2 being very close to $\lambda_1 = 1$, we will have dramatically slow convergence. As this is the main problem for all approaches to biomolecular dynamics and statistics, this is also a bottleneck of the transfer operator approach. An entire bunch of the literature aims at tackling this problem that is often called the *trapping problem* [4, 22]. In the framework of the transfer operator approach presented herein, A. Fischer recently designed a hierarchical approach tailored to accelerate convergence called *uncoupling-coupling* (UC) [23, 25]. Its *key assumption* is the following property of all stochastic systems designed to sample the canonical ensemble: Decreasing temperature induces stronger metastabilities, while metastability vanishes for large temperatures. Thus heating can help to reduce trapping which reappears if the system is annealed to lower temperatures. The uncoupling-coupling approach has been designed to circumvent this problems by combining the idea of domain decomposition with bridge sampling techniques.

In Section 8 a special bridge sampling technique called *Adaptive Temperature HMC* (ATHMC) [24] is used. Based on the Hybrid Monte Carlo procedure ATHMC reduces trapping problems by allowing to adapt the temperature during the sampling such that it can be increased to induce exits from metastable subsets. It was demonstrated that this procedure can be described by means of a generalized ensemble such that all parts of the sample (with different temperatures) can be reweighted to the temperature of interest [24].

14 Discretization in Higher Dimensions

Any discretization will suffer from the *curse of dimensionality* whenever it were based on uniform partition of all of the hundreds or thousands of degrees of freedom in a typical biomolecular system. Fortunately, chemical observations reveal that—even for larger biomolecules—the curse of dimensionality can be circumvented by exploiting the hierarchical structure of the dynamical and statistical properties of biomolecular systems: Firstly, only relatively few *conformational* or *essential degrees of freedom* are needed to describe the conformational transitions [1]. Furthermore, the canonical density has a rich spatial multiscale structure induced by the rich structure of the potential energy landscape. This structure induces a hierarchical cluster structure of the sampling data that can be identified and used to define a multilevel discretization adapted to the structures of the statistical data.

These observations give rise to a collection of approaches to the construction of *structure-adapted discretizations*:

Essential Degrees of Freedom. In the (low dimensional) subspace of essential degrees of freedom most of the positional fluctuations occur, while in the remaining degrees of freedom the motion can be considered as "physically constrained". Based on the available sampling, we may determine essential degrees of freedom either in the position space according to Amadei et al. [1] or in the space of internal degrees of freedom, e.g., dihedral angles, by statistical analysis of circular data [36]. Either case is based on a principal component analysis of the sampling. As shown in [36], this procedure may results in a enormous reduction of the number of degrees of freedom and, consequently, in a moderate number of subsets within the decomposition when discretizing the essential variables only. The principal component analysis is a linear approach to essential degrees of freedom. A characterization and identification of more general nonlinear essential degrees of freedom presently is a topic of further investigation.

Clustering Algorithms. Another approach of decomposing the state space is based on clustering the sampling data by means of clustering algorithms (see, e.g., [39] and cited references). These methods cluster the sampling data according to structural similarity: The set of sampling points is partitioned into disjoint subsets with the property that two states belonging to the same subset are in some sense structural closer to each other than two states belonging to different subsets. A crucial question is the design of appropriate measures of structural similarity. In the biomolecular application context, these measures may either be based on the Cartesian coordinates or on the internal degrees of freedom. In contrast to the former the latter approach is invariant under rotations and translations of the entire molecule.

A novel promising approach to the above type of clustering problem uses self–organizing maps, a special kind of neural networks. Self–organizing maps allow to cluster the sampling data by assigning each sampling point to its nearest "neurons", each of them representing a subset of the decomposition. We have demonstrated its successful application to sampling data of biomolecular systems in [30]. More advanced extensions, such as "box–neurons" and a hierarchical embedding, have recently been designed [28, 29].

Whenever the statistical distribution allows to be clustered into a limited but significant number of clusters (e.g. a few thousand at most), these clusters can be used to define a statistics-adapted discretization as by fuzzy partitions of unity or by introducing discretization "boxes" such that each box contains a single cluster; for an application to biomolecular systems see [36, 60].

Chapter 7. Illustrative Numerical Experiments

We now want to illustrate the transfer operator approach to metastability in application to different dynamical descriptions that are based on the earlier introduced perturbed three–well potential (see Figure 7, left). Further investigations, including dependence on parameters and discretization, can be found in [35]. The theoretical justification of the transfer operator approach via conditions (C1) and (C2) for the below dynamical descriptions can be found in [54, 35].

Parameters. The perturbed three–well potential is defined by

$$V(q) \;=\; \frac{1}{100}\left(q^6 - 30q^4 + 234q^2 + 14q + 100 + 30\sin(17q) + 26\cos(11q)\right).$$

Below, we analyze the ensemble dynamics based on the Hamiltonian system with randomized momenta, the Langevin system and the Smoluchowski system. We choose $\beta = 2.0$ for the inverse temperature and $\gamma = 2.0$ for the friction constant. Then, σ is defined via the relation $\beta = 2\gamma/\sigma^2$ as stated in eq. 2.6. For the observation time span we take $\tau = 1.0$.

Sampling. We sample the Markov processes given by the Hamiltonian system with randomized momenta with periodic boundary conditions on the positional state space $[-5, +5]$, the Langevin systems on $\mathbf{X} = \mathbf{R} \times \mathbf{R}$ and the Smoluchowski systems on $\mathbf{X} = \mathbf{R}$. The sampling length is $n = 300000$ points.

Discretization. We discretize the positional state space into $n = 70$ equally sized intervals (boxes). For the Langevin dynamics, we additionally have to discretize the space of momenta. Examining the canonical density of momenta

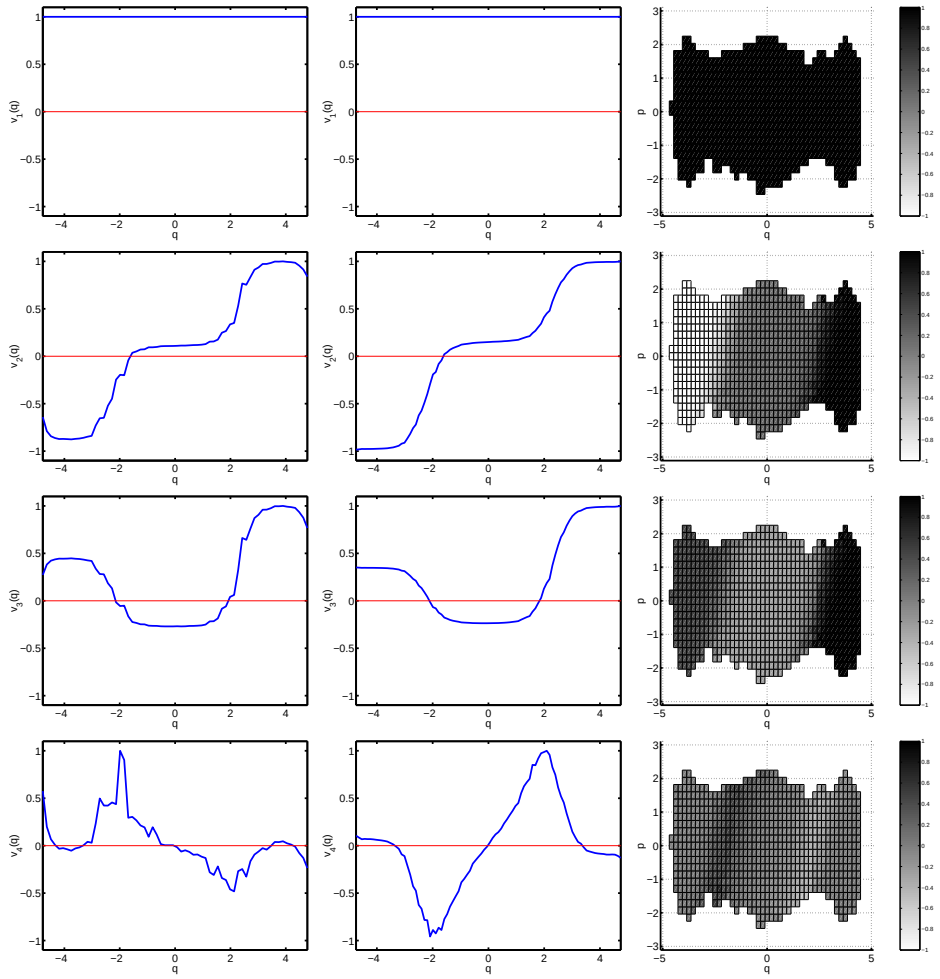

Fig. 13. *The four dominant eigenfunctions of the propagator P_τ for different model systems. Left: Hamiltonian system with randomized momenta corresponding to the eigenvalues* $1.0000, 0.9939, 0.9912, 0.6946$ *(from top to bottom). Middle: Smoluchowski equation for* $\gamma = 2.0$ *corresponding to the eigenvalues* $1.0000, 0.9925, 0.9893, 0.6585$. *Right: Langevin equation for* $\gamma = 2.0$ *corresponding to the eigenvalues* $1.0000, 0.9948, 0.9924, 0.6796$.

reveals that it is very unlikely to stay outside the interval $[-3, +3]$. Hence, we discretize the state space of momenta $\mathbf{R}$ by discretizing $[-3, +3]$ into 28 equally sized intervals and adding the two infinite intervals $(-\infty, -3)$ and $(3, \infty)$. Applying the discretization methods described in Section 6, we end up with an $n \times n$ stochastic transition matrix S with $n = 50 \times 30$ for the Langevin dynamics and $n = 70$ otherwise. For the Hamiltonian system with randomized momenta and the Smoluchowski dynamics, the transition matrix is self–adjoint.

Hamiltonian System with randomized momenta. Solving the eigenvalue

problem for S yields:

λ_1	λ_2	λ_3	λ_4	λ_5	λ_6	...
1.000	0.9939	0.9912	0.6946	0.6481	0.5952	...

Application of our identification algorithm yields a decomposition of the state space $\mathcal{D} = \{C_1, C_2, C_3\}$ with $C_1 = \{q \leq -2.13\}$, $C_2 = \{-2.13 < q \leq 1.99\}$ and $C_3 = \{1.99 < q\}$. The statistical weights $\mu(C_k)$ within the positional canonical ensemble μ and the metastabilities $p(C_k, C_k)$ are given by the following table:

metastable subset	C_1	C_2	C_3
statistical weight	0.2018	0.6979	0.1003
metastability	0.9883	0.9938	0.9800

The essential statistical behavior, i.e., the probability of transitions between the metastable subsets, is described by the coupling matrix $C = (c_{jk})_{j,k=1,2,3}$ with $c_{jk} = p(C_j, C_k)$. For our example, we obtain

$$C = \begin{pmatrix} 0.9883 & 0.0117 & 0 \\ 0.0034 & 0.9938 & 0.0029 \\ 0 & 0.0200 & 0.9800 \end{pmatrix}.$$

Langevin system. Solving the eigenvalue problem for S yields

λ_1	λ_2	λ_3	λ_4	λ_5	...
1.0000	0.9948	0.9924	0.6796	0.5365	...

Application of our identification algorithm yields a decomposition of the state space $\mathcal{D} = \{C_1, C_2, C_3\}$. The statistical weights $\mu(C_k)$ within the canonical ensemble μ and the metastabilities $p(C_k, C_k)$ are given by the following table:

metastable subset	C_1	C_2	C_3
statistical weight	0.1918	0.7012	0.1070
metastability	0.9887	0.9946	0.9851

(14.1)

Calculating the coupling matrix yields

$$C = \begin{pmatrix} 0.9887 & 0.0113 & 0 \\ 0.0031 & 0.9946 & 0.0023 \\ 0 & 0.0149 & 0.9851 \end{pmatrix}. \tag{14.2}$$

Smoluchowski system. Solving the eigenvalue problem for S yields:

λ_1	λ_2	λ_3	λ_4	λ_5	λ_6	...
1.0000	0.9925	0.9893	0.6585	0.5496	0.4562	...

Application of our identification algorithm yields a decomposition of the state space $\mathcal{D} = \{C_1, C_2, C_3\}$ with $C_1 = \{q \leq -2.04\}$, $C_2 = \{-2.04 < q \leq 1.94\}$ and $C_3 = \{1.94 < q\}$. The statistical weights $\mu(C_k)$ within the positional canonical ensemble μ and the metastabilities $p(C_k, C_k)$ are given by the following table:

metastable subset	C_1	C_2	C_3
statistical weight	0.2083	0.6936	0.0981
metastability	0.9863	0.9926	0.9770

The coupling matrix $C = (c_{jk})_{j,k=1,2,3}$ is given by

$$C = \begin{pmatrix} 0.9863 & 0.0137 & 0 \\ 0.0041 & 0.9926 & 0.0033 \\ 0 & 0.0230 & 0.9770 \end{pmatrix}.$$

Determining a decomposition of the state space following the Exit Time Approach and partitioning according to the zeros of the second or third eigenfunction v_2 and v_3, respectively, we obtain:

> Second eigenfunction: $\mathcal{D} = \{C_1, C_2\}$ with $C_1 = \{q \leq -1.32\}$ and $C_2 = \{-1.32 < q\}$ corresponding to the exit rate $\Gamma(C_i) = -\log(\lambda_2)/\tau = 0.0076$.
> Third eigenfunction: $\mathcal{D} = \{D_1, D_2, D_3\}$ with $D_1 = \{q \leq -2.04\}$, $D_2 = \{-2.04 < q \leq 1.94\}$ and $D_3 = \{1.94 < q\}$ corresponding to the exit rate $\Gamma(D_i) = -\log(\lambda_3)/\tau = 0.0107$.

Hence, in this case the decomposition induced by h_3 is identical to the decomposition obtained via the identification algorithm.

Chapter 8. Application to Biomolecular Systems

In this section we demonstrate that the algorithmic strategy presented in Section 7 can be applied to identify biomolecular conformations even for large systems as, for instance, small biomolecules with hundreds of atoms. For large systems, we have to face two particular problems:

(1) How to generate a sample of the stationary distribution in a high–dimensional space?
(2) How to decompose the highly–dimensional state space in order to discretize the propagator?

We will address these problems in the following.

Analyzing a Small Biomolecule. This section illustrates the performance of the algorithmic approach to the tri-ribonucleotide adenylyl(3'-5')cytidylyl(3'-5')cytidin (r(ACC)) model system in vacuum, see Figure 14. Its physical representation is based on the GROMOS96 extended atom force field [59], resulting in $N = 70$ atoms, hence $\Omega = \mathbf{R}^{210}$ and $\Gamma = \mathbf{R}^{420}$. The internal fluctuations are modeled w.r.t. the Hamiltonian system with randomized momenta. For details see [36].

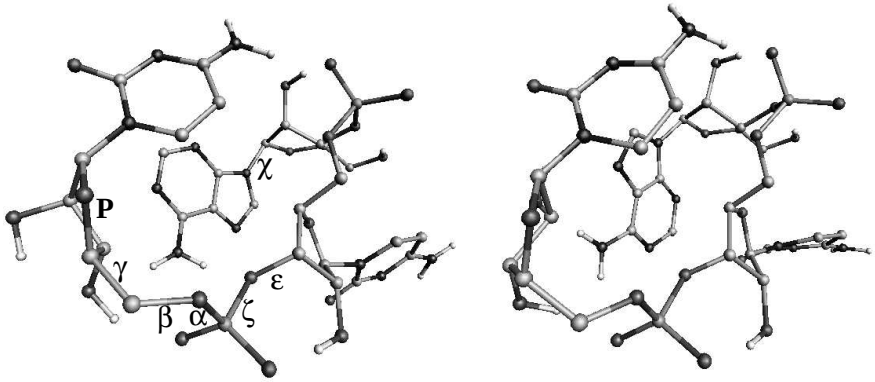

Fig. 14. *Two representatives of different conformations of r(ACC). Left: The χ angle around the first glycosidic bond is in* anti *position (-175 degrees) and the terminal ribose pucker P is in C(3')endo C(2')exo conformation. Right: The χ angle is in* syn *position (19 degrees) and the terminal ribose in C(2')endo C(3')exo conformation. Visualization by amira [2].*

The sampling of the canonical ensemble was generated using an adaptive temperature hybrid Monte Carlo method [24] at $T = 300$K resulting in the sampling sequence $q_1, \ldots, q_{32000} \in \Omega$. The dynamical fluctuations within the canonical ensemble were approximated by integrating $M = 4$ short trajectories of length $\tau = 80$fs starting from each sampling point. To facilitate transitions,

analogous to the ATHMC sampling, the momenta were chosen according to the canonical ensemble of momenta corresponding to four different temperatures between $300K - 400$K and reweighted afterwards. This resulted in a total of $4 \times 32.000 = 128.000$ trajectories.

The configurational space was discretized using all four essential degrees of freedom, which were identified by means of a statistical analysis of the sampling data (see [36]), resulting in $d = 36$ discretization subsets. Then the 36×36 stochastic transition matrix S was computed based on the 128.000 transitions taking the different weighting factors into account. The computation of the eigenvalues of S close to 1 yielded a cluster of eight eigenvalues with a significant gap to the remaining part of the spectrum, as shown in the following table:

k	1	2	3	4	5	6	7	8	9	...
λ_k	1.00	0.99	0.98	0.97	0.96	0.95	0.93	0.90	0.81	...

Finally, we computed conformations based on the corresponding eight eigenvectors of S via the identification algorithm presented in Section 8. We identified eight conformations; their statistical weights and metastabilities are shown in the following table:

conformations	C_1	C_2	C_3	C_4	C_5	C_6	C_7	C_8
statistical weight	0.11	0.01	0.12	0.03	0.32	0.04	0.29	0.10
metastability	0.99	0.94	0.96	0.89	0.99	0.95	0.98	0.96

The transition probabilities between the different conformations are visualized schematically in Figure 15. The matrix allows to define a hierarchy between the clusters: on the top level, there are two clusters, one consisting of the conformations $C_1, \ldots, C_4$ and the other consisting of the conformations $C_5, \ldots, C_8$. This structure corresponds to the two 4×4 blocks on the diagonal. On the next level, each of these clusters splits up into two subclusters yielding four conformations $\{C_1, C_2\}$, $\{C_3, C_4\}$, $\{C_5, C_6\}$, $\{C_7, C_8\}$. On the bottom level, each cluster is further divided resulting in eight conformations.

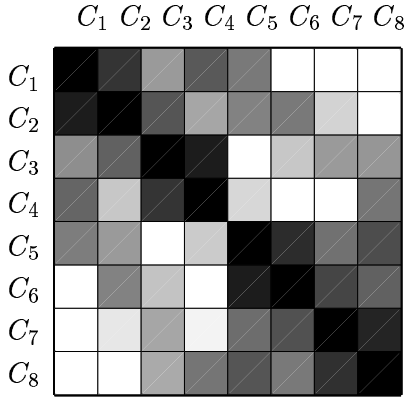

Fig. 15. *Schematical visualization of the transition probabilities $p(\tau, C_i, C_j)$ between the conformation C_i (row) and C_j (column). The colors are chosen according to the logarithm of the corresponding entries: from $p \approx 0$ (light) to $p \approx 1$ (dark).*

Chapter 9. Appendix

A Some Mathematical Aspects of Transfer Operators

Consider the state space $\mathbf{X} \subset \mathbf{R}^m$ for some $m \in \mathbf{N}$ equipped with the Borel σ–algebra $\mathcal{A}$ on $\mathbf{X}$. The evolution of a single microscopic system is supposed to be given by a homogeneous Markov process $X_t = \{X_t\}_{t \in \mathbf{T}}$ in continuous or discrete time with $\mathbf{T} = \mathbf{R}_0^+$ or $\mathbf{T} = \mathbf{N}$, respectively. The motion of X_t is given in terms of a stochastic transition function p according to

$$p(t, x, A) \;=\; \mathbf{P}[X_{t+s} \in A \;|X_s = x],$$

for every $t, s \in \mathbf{T}$, $x \in \mathbf{X}$ and $A \subset \mathbf{X}$. The map $p : \mathbf{T} \times \mathbf{X} \times \mathcal{B}(\mathbf{X}) \to [0, 1]$ has the following properties

(i) $x \mapsto p(t, x, A)$ is measurable for every $t \in \mathbf{T}$ and $A \in \mathcal{B}(\mathbf{X})$,
(ii) $A \mapsto p(t, x, A)$ is a probability measure for every $t \in \mathbf{T}$ and $x \in \mathbf{X}$.
(iii) $p(0, x, \mathbf{X} \setminus \{x\}) = 0$ for every $x \in \mathbf{X}$.
(iv) the Chapman–Kolmogorov equation

$$p(t + s, x, A) \;=\; \int_{\mathbf{X}} p(t, x, \mathrm{d}z)\; p(s, z, A)$$

holds for every $t, s \in \mathbf{T}$, $x \in \mathbf{X}$ and $A \subset \mathbf{X}$.

The relation between Markov processes and stochastic transition functions is one–to–one, i.e., every homogeneous Markov process defines a stochastic transition function satisfying properties (i) to (iv), and vice versa [48, Chapter 3].

To introduce the transfer operators consider the Banach spaces of equivalence classes of measurable functions

$$L^r(\mu) \;=\; \left\{u : \mathbf{X} \to \mathbf{C} : \int_{\mathbf{X}} |u(x)|^r \mu(\mathrm{d}x) < \infty\right\}. \tag{A.1}$$

for $1 \leq r < \infty$ and

$$L^\infty(\mu) \;=\; \left\{u : \mathbf{X} \to \mathbf{C} : \mu\text{-ess}\sup_{x\in\mathbf{X}} |u(x)| < \infty\right\}$$

with corresponding norms $\|\cdot\|_r$ and $\|\cdot\|_\infty$, respectively. Due to Hölder's inequality we have $L^r(\mu) \subset L^s(\mu)$ for every $1 \leq s \leq r \leq \infty$. The propagators or forward transfer operators $P^t : L^1(\mu) \to L^1(\mu)$ are defined by

$$P^t v(y)\; \mu(\mathrm{d}y) \;=\; \int_{\mathbf{X}} p(t,x,\mathrm{d}y) v(x) \mu(\mathrm{d}x),$$

while the backward transfer operators $T^t : L^\infty(\mu) \to L^\infty(\mu)$ are given by

$$T^t u(x) \;=\; \mathsf{E}_x[u(X_t)] \;=\; \int_{\mathbf{X}} u(y) p(t,x,\mathrm{d}y).$$

The assumed invariance of μ w.r.t. the stochastic transition function guarantees that the forward transfer operators is well–defined [51, Chapter 4] and may be consider as acting on $L^r(\mu)$ for $1 \leq r$. Moreover the backward transfer operator may be extended to any $L^r(\mu)$ with $1 \leq r$.

Due to the properties of the stochastic transition function p both definitions define semigroups of Markov operators, i.e., we especially have

$$T^t T^s \;=\; T^{t+s} \quad \text{and} \quad P^t P^s = P^{s+t},$$

and both operators, $A = T^t$ or $A = P^t$, conserve norm $\|Av\|_1 = \|A\|_1$ and positivity $Av \geq 0$ if $v \geq 0$. With the duality bracket defined in (6.6) the backward transfer operator is the adjoint of the propagator: $(P^t)^* = T^t$. Since $L^1(\mu)$ is a proper subset of the dual of $L^\infty(\mu)$, we have $P^t \subsetneq (T^t)^*$, hence P^t is not the adjoint of T^t. As a consequence, it is much easier to relate properties of P^t to T^t than vice versa.

Spectral Properties. Consider a complex Banach space E with norm $\|\cdot\|$ and denote the spectrum[4] of a bounded linear operator $P : E \to E$ by $\sigma(P)$. For an eigenvalue $\lambda \in \sigma(P)$, the multiplicity of λ is defined as the dimension of the generalized eigenspace; see e.g., [41, Chap. III.6]. Eigenvalues of multiplicity 1 are called simple. The set of all eigenvalues $\lambda \in \sigma(P)$ that are isolated and of finite multiplicity is called the **discrete spectrum**, denoted by $\sigma_{\text{discr}}(P)$. The **essential spectral radius** $r_{\text{ess}}(P)$ of P is defined as the smallest real

[4] For common functional analytical terminology see, e.g., [19, 33, 41, 61].

number, such that outside the ball of radius $r_{\text{ess}}(P)$, centered at the origin, are only discrete eigenvalues, i.e.,

$$r_{\text{ess}}(P) \;=\; \inf\{r \geq 0 : \lambda \in \sigma(P) \text{ with } |\lambda| > r \text{ implies } \lambda \in \sigma_{\text{discr}}(P)\}.$$

This definition of $r_{\text{ess}}(P)$ is unusual in the sense that it does not involve any definition of the essential spectrum. This is owed to the surprising fact that although there are many different definitions of essential spectra, the associated spectral radii coincide [35, 44] and are therefore somehow independent of the specific definition of essential spectra.

Proposition A.1 ([35]) *Consider the* ***Lebesgue decomposition*** *of the stochastic transition function*

$$p(x, \mathrm{d}y) \;=\; p_a(x, y)\mu(\mathrm{d}y) + p_s(x, \mathrm{d}y)$$

where p_a and p_s represent the absolutely continuous and the singular part w.r.t. μ, respectively. Assume that

(i) the inequality

$$\int_{\mathbf{X}} \int_{\mathbf{X}} p_a(x, y)^2 \mu(\mathrm{d}x)\mu(\mathrm{d}y) \;<\; \infty$$

holds, and

(ii) there exists some $\eta < 1$ such that

$$\eta \;=\; \sup p_s(x, \mathbf{X}) \;=\; 1 - \inf \int_{\mathbf{X}} p_a(x, y)\mu(\mathrm{d}y).$$

for μ–a.e. $x \in \mathbf{X}$.

Then, the essential spectrum is uniformly bounded away from 1, more precisely, we have $r_{\text{ess}}(P) < \sqrt{\eta} < 1$. In particular, condition (C1) is fulfilled.

As stated in Section 7 the probabilistic interpretation of condition (C2) is that the Markov process admits a *unique* invariant probability measure and is *aperiodic*, hence does not show any periodic behavior. Consequently, the state space $\mathbf{X}$ can neither be decomposed into non–interacting (invariant) subsets nor into so–called cyclic subset such that the Markov process cycles with probability 1 along these cyclic subset. To interpret condition (C1), consider the Lebesgue decomposition of the stochastic transition function p. For simplicity assume that the invariant measure μ is absolutely continuous w.r.t. the Lebesgue measure as, for instance, the measure induced by the canonical ensemble. Then, as shown in Propositon A.1, the essential spectral radius $r_{\text{ess}}(P)$ is related to regularity conditions on the stochastic transition function. The essential spectral radius is close to one, if (a) the singular part p_s is close to one, or (b) the absolutely continuous part p_a shows a singularity like behavior,

e.g., grows too fast at infinity. There is a rapidly growing literature on testable conditions, which imply that neither (a) nor (b) are valid and thus the spectral radius is strictly bounded away from 1 []. We only want to make the following remarks: Firstly, for the special case of the deterministic Hamiltonian system, the absolutely continuous part p_a vanishes such that $r_{\mathrm{ess}}(P) = 1$ via condition (a). Then, for the case of Langevin or Smoluchowski dynamics with smooth potentials, the singular part vanishes and the validity of condition (C1) depends on the growths of p_a at infinity only; therefore Ljapunov conditions on p_a suffice to prove (C1) in these cases. Finally, we can safely exclude problems with condition (a) whenever the transition function p allows to reach an open set with positive measure w.r.t. μ from any point $x \in \mathbf{X}$. This shows that for the Hamiltonian system with randomized momenta we only have to exclude that there is an initial position q from which τ-trajectories with arbitrary initial momentum always end up in some discrete set of positions. This typically is not the case such that condition (a) will typically be no problem for the Hamiltonian system with randomized momenta whereas it is for the deterministic Hamiltonian system, see [54] for details.

Implications of $\mathcal{V}$–uniform ergodicity. The main body of ergodic theory and spectral theory of transfer operators is based upon another vector space setting developed in [48, Chapter 16]. Let $\mathcal{V} : \mathbf{X} \to [1, \infty)$, finite a.e., be a given Ljapunov function, and denote by $L^\infty(\mathcal{V})$ the vector space of measurable functions $h : \mathbf{X} \to \mathbf{C}$ satisfying

$$\|h\|_\mathcal{V} \;=\; \sup_{x \in \mathbf{X}} \frac{|h(x)|}{\mathcal{V}(x)} < \infty.$$

Let $\|\cdot\|_\mathcal{V}$ also denote the operator norm induced by this $\mathcal{V}$–norm. The $\mathcal{V}$–norm on measures (as it is used in Section 8) is defined by

$$\|\nu\|_\mathcal{V} \;=\; \sup_{|v| \leq \mathcal{V}} |\int_\mathbf{X} v(x)\nu(\mathrm{d}x)|,$$

where $|v| \leq \mathcal{V}$ is understood to hold pointwise for every measurable function v and every $x \in \mathbf{X}$; here $\mathcal{V}$ needs to be integrable. For the special case $\mathcal{V} \equiv 1$, the $\mathcal{V}$–norm coincides with the total variation norm $\|\cdot\|_{\mathrm{TV}}$.

Consider the backward transfer operator acting on the function space $L^\infty(\mathcal{V})$. We have seen in Section 9 that the assumption of $\mathcal{V}$–ergodicity is crucial for our approach. Then, from Theorem 5.2 of [18] and the results of [37] it follows

Theorem A.2 *If the stochastic transition function p is $\mathcal{V}$–uniformly ergodic then,*

(1) there is an invariant probability measure μ, and the semigroup T^t strongly converges in $L^\infty_\mathcal{V}$.

(2) T^t *admits a spectral gap in* $L^\infty(\mathcal{V})$*, i.e., the set* $\sigma(T^t) \cap \{z \in \mathbf{C} : |z-1| \leq \epsilon\}$ *is finite for sufficiently small* $\epsilon > 0$*.*

(3) for any $B \in \mathcal{B}$ *with* $\mu(B) > 0$*, there exists* $\bar{\Gamma}_B > 0$ *and* $b < \infty$ *such that*

$$\mathbf{P}_x\{\varrho_B \geq t\} \leq b\,\mathcal{V}(x)\,e^{-\bar{\Gamma}_B t}, \qquad x \in \mathbf{X}. \tag{A.2}$$

The last properties nicely illustrates that there is a deep connection between $\mathcal{V}$–ergodicity, the existence of a spectral gap, and the exponential decay of the exit time distribution. This is important for the definition of exit rates in the next subsection.

B Definition of Exit Rates

Consider the Markov process X_t with transition function p. As outlined above, p defines the semigroup of transfer operators via $T^t u(x) = \mathsf{E}_x[u(X_t)]$. We now turn our attention to some open connected set B and define the **restricted process** on B induced by the process X_t via the semigroup of restricted transfer operators

$$T_B^t u(x) = \mathsf{E}_x[u(X_t)\mathbf{1}_X(\varrho_{B^c} \geq t)],$$

where ϱ_{B^c} denotes the exit time from B^c as introduced in (5.1). Thus, the new process lives on B only; considering the original process exits from B are killed. The family $\{T_B^t\}$ is a semigroup of positive operators that in general are no longer Markov operators. We define the spectral radius for the family $\{T_B^t\}$ by

$$r(\{T_B^t\}) = \lim_{t\to\infty} (\|T_B^t\|_\mathcal{V})^{1/t},$$

and define the $\mathcal{V}$–**exit rate** from the set B by

$$\Gamma(B) = -\log r(\{T_B^t\}).$$

Now, one may raise the question whether the so-defined exit rate really measures the asymptotic decay of the distribution of exit times in the sense of Section 5. The answer is yes: If for the set B the exit time distribution decays due to (5.2) for some $\Gamma > 0$ that is constant in B, then $\|T^t\|_\mathcal{V}$ decays asymptotically as $c\exp(-\Gamma t)$ such that $\Gamma(B) = -\log r(\{T_B^t\}) = \Gamma$. The other way around and in terms of a rigorous statement for the situation described in Section 9, we have:

Theorem B.1 *Suppose that the conditions of Theorem 9.2 hold implying that the subset* C *is metastable with exit rate* $\Gamma > 0$*. Then there exists* $\delta_0 > 0$ *such*

that for all $s, T > 0$ the conditional distribution of exit times satisfies

$$F_x(s,T) \;=\; e^{-\Gamma s}\left[\frac{1+O(G_x(s))}{1+O\left(e^{-T\delta_0}G_x(s)\right)}\right], \qquad (T\to\infty)$$

with $G_x(s) = e^{-\delta_0 s}\mathcal{V}(x)/h(x)$.

In [37], δ_0 is some well-defined computable constant and it is shown that in typical situations we have $\delta_0 \gg \Gamma$.

References

[1] A. Amadei, A. B. M. Linssen, and H. J. C. Berendsen. Essential dynamics of proteins. *Proteins*, 17:412–425, 1993.

[2] Amira—advanced visualization, data analysis and geometry reconstruction, user's guide and reference manual. Konrad-Zuse-Zentrum für Informationstechnik Berlin (ZIB), Indeed–Visual Concepts GmbH and TGS Template Graphics Software Inc., 2000.

[3] B. J. Berne, G. Ciccotti, and D. F. Coker, editors. *Classical and Quantum Dynamics in Condensed Phase Simulations.* Singapure: World Scientific, 1998.

[4] B. J. Berne and J. E. Straub. Novel methods of sampling phase space in the simulation of biological systems. *Curr. Opinion in Struct. Biol.*, 7:181–189, 1997.

[5] P. G. Bolhuis, C. Dellago, D. Chandler, and P. Geissler. Transition path sampling: Throwing ropes over mountain passes, in the dark. *Ann. Rev. of Phys. Chem.*, in press, 2001.

[6] S. D. Bond and B. B. L. Benedict J. Leimkuhler. The Nosé–Poincaré method for constant temperature molecular dynamics. *JCP*, 151(1):114–134, 1999.

[7] A. Bovier, M. Eckhoff, V. Gayrard, and M. Klein. Metastability in stochastic dynamics of disordered mean–field models. *Probab. Theor. Rel. Fields*, 119:99–161, 2001.

[8] D. Chandler. Finding transition pathways: throwing ropes over rough montain passes, in the dark. In B. Berne, G. Ciccotti, and D. Coker, editors, *Classical and Quantum Dynamics in Condensed Phase Simulations*, pages 51–66. Singapure: World Scientific, 1998.

[9] E. B. Davies. Metastable states of symmetric Markov semigroups I. *Proc. London Math. Soc.*, 45(3):133–150, 1982.

[10] M. Dellnitz and O. Junge. An adaptive subdivision technique for the approximation of attractors and invariant measures. *Comput. Visual. Sci.*, 1:63–68, 1998.

[11] M. Dellnitz and O. Junge. On the approximation of complicated dynamical behavior. *SIAM J. Num. Anal.*, 36(2):491–515, 1999.

[12] P. Deuflhard and F. Bornemann. *Numerische Mathematik II.* de Gruyter, 1994.

[13] P. Deuflhard, M. Dellnitz, O. Junge, and C. Schütte. Computation of essential molecular dynamics by subdivision techniques. In *[15]*, pages 98–115, 1999.

[14] P. Deuflhard, T. Friese, and F. Schmidt. A nonlinear multigrid eigenproblem

solver for the complex Helmholtz equation. Preprint SC-97-55, Konrad–Zuse–Zentrum, Berlin. Available via http://www.zib.de/bib/pub/pw/, 1997.

[15] P. Deuflhard, J. Hermans, B. Leimkuhler, A. E. Mark, S. Reich, and R. D. Skeel, editors. *Computational Molecular Dynamics: Challenges, Methods, Ideas*, volume 4 of *Lecture Notes in Computational Science and Engineering*. Springer, 1999.

[16] P. Deuflhard and A. Hohmann. *Numerische Mathematik I.* de Gruyter, Berlin, 1993.

[17] P. Deuflhard, W. Huisinga, A. Fischer, and C. Schütte. Identification of almost invariant aggregates in reversible nearly uncoupled Markov chains. *Lin. Alg. Appl.*, 315:39–59, 2000.

[18] D. Down, S. P. Meyn, and R. L. Tweedie. Exponential and uniform ergodicity of Markov processes. *Ann. Prob.*, 23:1671–1691, 1995.

[19] N. Dunford and J. T. Schwartz. *Linear Operators, Part I: General Theory*, volume VII of *Pure and Applied Mathematics*. Interscience, New York, 1957.

[20] W. E, W. Ran, and E. Vanden-Eijnden. Probing multiscale energy landscapes using the string method. *Phys. Rev. Lett.*, submitted, 2002.

[21] R. Elber and M. Karplus. Multiple conformational states of proteins: A molecular dynamics analysis of Myoglobin. *Science*, 235:318–321, 1987.

[22] D. M. Ferguson, J. I. Siepmann, and D. G. Truhlar, editors. *Monte Carlo Methods in Chemical Physics*, volume 105 of *Advances in Chemical Physics*. Wiley, New York, 1999.

[23] A. Fischer. An uncoupling–coupling technique for Markov chains Monte Carlo methods. Konrad–Zuse–Zentrum, Berlin. Report 00-04, 2000.

[24] A. Fischer, F. Cordes, and C. Schütte. Hybrid Monte Carlo with adaptive temperature in a mixed–canonical ensemble: Efficient conformational analysis of RNA. *J. Comput. Chem.*, 19:1689–1697, 1998.

[25] A. Fischer, C. Schütte, P. Deuflhard, and F. Cordes. Hierarchial uncoupling–coupling of metastable conformations. In T. Schlick and H. H. Gan, editors, *Computational Methods for Macromolecules: Challenges and Applications, Proceedings of the 3rd International Workshop on Algorithms for Macromolecular Modelling, New York, Oct. 12-14, 2000*, volume 24 of *Lecture Notes in Computational Science and Engineering*. Springer, 2002.

[26] H. Frauenfelder and B. H. McMahon. Energy landscape and fluctuations in proteins. *Ann. Phys. (Leipzig)*, 9(9–10):655–667, 2000.

[27] H. Frauenfelder, P. J. Steinbach, and R. D. Young. Conformational relaxation in proteins. *Chem. Soc.*, 29A(145–150), 1989.

[28] T. Galliat and P. Deuflhard. Adaptive hierarchical cluster analysis by self-organizing box maps. Konrad–Zuse–Zentrum, Berlin. Report SC-00-13, 2000.

[29] T. Galliat, P. Deuflhard, R. Roitzsch, and F. Cordes. Automatic identification of metastable conformations via self–organized neural networks. In T. Schlick and H. H. Gan, editors, *Computational Methods for Macromolecules: Challenges and Applications, Proceedings of the 3rd International Workshop on Algorithms for Macromolecular Modelling, New York, Oct. 12-14, 2000*, volume 24 of *Lecture Notes in Computational Science and Engineering*. Springer, 2002.

[30] T. Galliat, W. Huisinga, and P. Deuflhard. Self-organizing maps combined

with eigenmode analysis for automated cluster identification. In H. Bothe and R. Rojas, editors, *Neural Computation*, pages 227–232. ICSC Academic Press, 2000.

[31] W. Gilks, S. Richardson, and D. Spiegelhalter, editors. *Markov chain Monte-Carlo in Practice*. Chapman and Hall, London, 1997.

[32] H. Grubmüller. Predicting slow structural transitions in macromolecular system: Conformational flooding. *1995*, 52:2893–2906, Phys. Rev. E.

[33] H. Heuser. *Funktionalanalysis*. Teubner, Stuttgart, 1986.

[34] T. Huber, A. E. Torda, and W. F. van Gunsteren. Local elevation: A method for improving the searching properties of molecular dynamics simulation. *JCAMD*, 8:695–708, 1994.

[35] W. Huisinga. *Metastability of Markovian systems: A transfer operator approach in application to molecular dynamics*. PhD thesis, Free University Berlin, 2001.

[36] W. Huisinga, C. Best, R. Roitzsch, C. Schütte, and F. Cordes. From simulation data to conformational ensembles: Structure and dynamic based methods. *J. Comp. Chem.*, 20(16):1760–1774, 1999.

[37] W. Huisinga, S. Meyn, and C. Schütte. Phase transitions & metastability in Markovian and molecular systems. Submitted, 2002.

[38] W. Huisinga and B. Schmidt. Metastability and Dominant Eigenvalues of Transfer Operators, in preparation, 2002.

[39] A. K. Jain and R. C. Dubes. *Algorithms for Clustering Data*. Prentice Hall, New Jersey, Advanced Reference Series edition, 1988.

[40] I. Karatzas and S. E. Shreve. *Brownian Motion and Stochastic Calculus*. Graduate Texts in Mathematics. Springer, New York, 1991.

[41] T. Kato. *Perturbation Theory for Linear Operators*. Springer, Berlin, 1995. Reprint of the 1980 edition.

[42] R. Kleeman. Measuring dynamical prediction utility using relative entropy. *Journ. Atmos. Sci.*, accepted, 2001.

[43] A. Lasota and M. C. Mackey. *Chaos, Fractals and Noise*, volume 97 of *Applied Mathematical Sciences*. Springer, New York, 2nd edition, 1994.

[44] A. Lebow and M. Schechter. Semigroups of operators and measures of non-compactness. *J. Funct. Anal.*, 7:1–26, 1971.

[45] R. B. Lehoucq, D. C. Sorensen, and C.Yang. *ARPACK User's Guide: Solution of Large Eigenvalue Problems by Implicit Restartet Arnoldi Methods*. Rice University, Houston, 1998.

[46] P. Lezaud. Chernoff and Berry–Esséen inequalities for Markov processes. *ESIAM: P & S*, 5:183–201, 2001.

[47] J. Mattingly, A. M. Stuart, and D. J. Higham. Ergodicity for SDEs and approximations: Locally Lipschitz vector fields and degenerated noise. Submitted, 2001.

[48] S. Meyn and R. Tweedie. *Markov Chains and Stochastic Stability*. Springer, Berlin, 1993.

[49] G. U. Nienhaus, J. R. Mourant, and H. Frauenfelder. Spectroscopic evidence for conformational relaxation in Myoglobin. *PNAS*, 89:2902–2906, 1992.

[50] R. Olender and R. Elber. Calculation of classical trajectories with a very large time step: Formalism and numerical examples. *J. Chem. Phys.*, 105:9299–9315, 1996.

[51] D. Revuz. *Markov Chains.* North–Holland, Amsterdam, Oxford, 1975.

[52] H. Risken. *The Fokker-Planck Equation.* Springer, New York, 2nd edition, 1996.

[53] G. O. Roberts and J. S. Rosenthal. Geometric ergodicity and hybrid Markov chains. *Elect. Comm. in Probab.*, 2:13–25, 1997.

[54] C. Schütte. *Conformational Dynamics: Modelling, Theory, Algorithm, and Application to Biomolecules.* Habilitation Thesis, Fachbereich Mathematik und Informatik, Freie Universität Berlin, 1998.

[55] C. Schütte, A. Fischer, W. Huisinga, and P. Deuflhard. A direct approach to conformational dynamics based on hybrid Monte Carlo. *J. Comput. Phys., Special Issue on Computational Biophysics*, 151:146–168, 1999.

[56] C. Schütte and W. Huisinga. On conformational dynamics induced by Langevin processes. In B. Fiedler, K. Gröger, and J. Sprekels, editors, *EQUADIFF 99 - International Conference on Differential Equations*, volume 2, pages 1247–1262, Singapore, 2000. World Scientific.

[57] C. Schütte, W. Huisinga, and P. Deuflhard. Transfer operator approach to conformational dynamics in biomolecular systems. In B. Fiedler, editor, *Ergodic Theory, Analysis, and Efficient Simulation of Dynamical Systems*, pages 191–223. Springer, 2001.

[58] G. Singleton. Asymptotically exact estimates for metatstable Markov semigroups. *Quart. J. Math. Oxford*, 35(2):321–329, 1984.

[59] W. F. van Gunsteren, S. R. Billeter, A. A. Eising, P. H. Hünenberger, P. Krüger, A. E. Mark, W. R. P. Scott, and I. G. Tironi. *Biomolecular Simulation: The GROMOS96 Manual and User Guide.* vdf Hochschulverlag AG, ETH Zürich, 1996.

[60] M. Weber and T. Galliat. Characterization of transition states in conformational dynamics using Fuzzy sets. Technical Report Report 02-12, Konrad–Zuse–Zentrum (ZIB), Berlin, March 2002.

[61] D. Werner. *Funktionalanalysis.* Springer, Berlin, 2nd edition, 1997.

[62] A. H. Zewail. Der Augenblick der Molekülbildung. *Spektrum der Wissenschaft, Digest 2: Moderne Chemie*, pages 18–26, 1995.

[63] A. H. Zewail. Femtochemistry: Recent progress in studies of dynamics and control of reactions and their transition state. *J. Phys. Chem.*, 100(31):12701–12724, 1996.

[64] H. X. Zhou, S. T. Wlodec, and J. A. McCammon. Conformation gating as a mechanism for enzyme specificity. *Proc. Nat. Acad. Sci. USA*, 95(9280–9283), 1998.